A TRIDENT SCHOLAR PROJECT REPORT

NO. 204

"Interleukin-2 Signal Transduction: A Diffusion-Kinetics Model"

UNITED STATES NAVAL ACADEMY
ANNAPOLIS, MARYLAND

U.S.N.A. - Trident Scholar project report; no. 204 (1993)

"Interleukin-2 Signal Transduction: A Diffusion-Kinetics Model"

by
Midshipman Michael P. Keith, Class of 1993
U.S. Naval Academy
Annapolis, Maryland

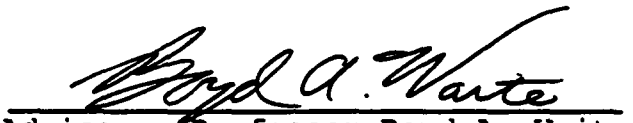

Adviser: Professor Boyd A. Waite
Chemistry Department

Accepted for Trident Scholar Committee

Chair

May 17, 1993

Date

REPORT DOCUMENTATION PAGE

Form Approved
OMB no. 0704-0188

1. AGENCY USE ONLY (Leave blank)	2. REPORT DATE	3. REPORT TYPE AND DATES COVERED
	May 17, 1993	

4. TITLE AND SUBTITLE
Interleukin-2 signal transduction : a diffusion-kinetics model

5. FUNDING NUMBERS

6. AUTHOR(S)
Michael Patrick Keith

7. PERFORMING ORGANIZATIONS NAME(S) AND ADDRESS(ES)
U.S. Naval Academy, Annapolis, MD

8. PERFORMING ORGANIZATION REPORT NUMBER
U.S.N.A. - Trident scholar project report ; no. 204

9. SPONSORING/MONITORING AGENCY NAME(S) AND ADDRESS(ES)

10. SPONSORING/MONITORING AGENCY REPORT NUMBER

11. SUPPLEMENTARY NOTES
Accepted by the U.S. Trident Scholar Committee

12a. DISTRIBUTION/AVAILABILITY STATEMENT
This document has been approved for public release; its distribution is UNLIMITED.

12b. DISTRIBUTION CODE

13. ABSTRACT (Maximum 200 words)

The diffusion-kinetics model for the interactions between interleukin-2 and each of its T-cell surface receptors (IL-2α and IL-2β) is presented. This model is unique in that it considers both three dimensional ligand-receptor interactions and two dimensional interactions between cell surface-bound species. Elementary rate laws are developed for initial encounters, rebounding interactions, and dissociations of free ligands and receptors according to the method of Waite[1] and Waite and Stewart[2]. Analogous rate laws are written for membrane bound species which undergo similar initial associations, rebounding interactions, and dissociations. A set of kinetic equations is proposed for a system consisting of two independent monovalent receptors and one monovalent ligand, simulating the interaction of the IL-2α and IL-2β receptors of the human T-cell with the lymphokine interleukin-2. Autocrine and paracrine growth and combinations of the two are studied by modifying the appropriate experimental parameters. Experimental associative and dissociative rate constants are determined for important T-cell surface species.

14. SUBJECT TERMS	15. NUMBER OF PAGES
Interleukin-2, diffusion, signalling, kinetics	91
	16. PRICE CODE

17. SECURITY CLASSIFICATION OF REPORT	18. SECURITY CLASSIFICATION OF THIS PAGE	19. SECURITY CLASSIFICATION OF ABSTRACT	20. LIMITATATION OF ABSTRACT
UNCLASSIFIED	UNCLASSIFIED	UNCLASSIFIED	UNCLASSIFIED

Abstract

The diffusion-kinetics model for the intera tween interleukin-2 and each of its T-cell surface receptors (IL-2α and IL-2β) is presented. This model is unique in that it considers both three dimensional ligand-receptor interactions and two dimensional interactions between cell surface-bound species. Elementary rate laws are developed for initial encounters, rebounding interactions, and dissociations of free ligands and receptors according to the method of Waite [1] and Waite and Stewart[2]. Analogous rate laws are written for membrane bound species which undergo similar initial associations, rebounding interactions, and dissociations. A set of kinetic equations is proposed for a system consisting of two independent monovalent receptors and one monovalent ligand, simulating the interaction of the IL-2α and IL-2β receptors of the human T-cell with the lymphokine interleukin-2. Autocrine and paracrine growth and combinations of the two are studied by modifying the appropriate experimental parameters. Experimental associative and dissociative rate constants are determined for important T-cell surface species.

keywords: Interleukin-2, diffusion, signalling, kinetics

Contents

1 Background

The cellular membrane is the barrier of the cell at which many biologically important interactions take place. These interactions include transport of materials in and out of the cell and the transduction of signals to the cell [3]. This signal transduction instructs the cell to replicate, synthesize a compound, etc.

Under the currently accepted fluid mosaic model [4], the cellular membrane consists of a phospholipid bilayer with the hydrophilic heads pointing outward and the hydrophobic tails on the inside, making a waterproof barrier. Many proteins can be associated with this lipid bilayer through various weak bonding interactions. Receptors are proteins that are in effect solvated in the cellular membrane and held in place by weak hydrophilic interactions, whereby nonpolar parts of the protein molecule interact with the hydrophobic portion of the cellular membrane. The actual receptor site of the protein molecule is a region with a special shape that exists on the outside of the cellular membrane. The entire receptor molecule, being solvated in the lipid bilayer, is free to diffuse in two dimensions and randomly does so, in search of the specific substrate for that site. The substrate may be a ligand diffusing towards the cell surface in the extra-cellular medium, or it may be bound to another receptor diffusing within the two-dimensional membrane.

The interaction of T-cells and the lymphokine interleukin-2 (IL-2) is one such

receptor-substrate interaction. The T-cells are key participants in the cell-mediated immune response of the body, and their action is mediated by interleukin-2.

When a T-cell is presented an antigen and recognizes it through a signal transduced through the cellular membrane, it begins to produce the lymphokine interleukin-2, which is a molecular communicator and growth factor for various cells of the immune system [5]. Interleukin-2 is necessary for the continued growth of the T-helper cell and for the growth of the T-cytotoxic cell which lyses cells containing the antigen [6, 7].

The growth of T-cells can be initiated by interleukin-2 in one of two fashions. In autocrine growth, interleukin-2 produced by a particular T-cell becomes bound to the IL-2 receptors on that same cell, causing it to continue its growth and production of interleukin-2. The interleukin-2 produced by a particular T-cell may also escape this cell's surface and enters the bulk solution. From there it may bind to the IL-2 receptors of another T-cell, causing it to grow and produce interleukin-2. This is known as paracrine growth [8].

In actual biological systems T-cell growth most likely occurs by some combination of these two methods. Both the autocrine and paracrine growth mechanisms are of interest here because they increase the number of cells which can recognize and defend against a specific antigen.

The nature of intracellular signaling is not of interest to this study. Only the kinetics of association and dissociation of interleukin-2 and its T-cell receptors that

lead to the signal transduction are significant to this study. The molecular signal that is generated once the interleukin-2-receptor complex is formed is also not of interest here.

It is currently believed that the IL-2 receptor is not merely a single protein but rather two proteins that must both be bound to interleukin-2 in order to stimulate the continued production of interleukin-2 and the growth of T-cells [9]. The interleukin-2 receptor is believed to consist of two proteins [10], the receptor (IL-2α), which is a protein with a molecular weight of $55kD$, and the receptor (IL-2β), which is a protein with a molecular weight of $75kD$. It is interesting to note that these receptors themselves do not appear until the T-cell has been activated by an antigen becoming bound to the T-cell [11]. It is known [12, 13] that IL-2α is a low-affinity receptor for interleukin-2, having a K_d of $1x10^{-8}M$ and that IL-2β is a medium-affinity receptor for interleukin-2, having a K_d of $1x10^{-9}M$. It is also known that interleukin-2 rapidly associates and dissociates with IL-2α but associates and dissociates slowly with IL-2β [10].

The actual signal transduction occurs when interleukin-2 is bound to both the IL-2α receptor and the IL-2β receptor, forming a ligand-receptor complex [5]. It is interesting to note, however, that interleukin-2 binds rapidly to the complex and yet dissociates slowly from the complex [10].

The objective of the current study is to quantitatively study the proposed mechanisms for receptor-ligand signaling in the IL-2 problem. There is an ongoing debate

over which mechanism is the correct model for the formation of the interleukin-2-T-cell surface receptors complex.

The affinity conversion mechanism for the interaction of T- cells and interleukin-2 is explained as follows. Interleukin-2 produced by an activated T-cell that is wandering in solution encounters an IL-2 receptor that is moving randomly in the two-dimensional cellular membrane. If the IL-2 has correct orientation and energy, all of which can be accounted for in a single association probability parameter, it will rapidly bind to the IL-2 receptor. This portion of the complex continues to be anchored in the cellular membrane by IL-2 and will move randomly within the membrane. If the interleukin-2/receptor complex, while diffusing randomly in the cell membrane, encounters the opposite type of IL-2 receptor with sufficient energy and proper orientation then the complete interleukin-2 - receptor complex is formed and an intracellular signal is transmitted, instructing the T-cell to begin producing more IL-2 and increase its rate of growth. The affinity of the IL-2α receptor is effectively converted to that of the IL-2β receptor when the complex is formed in this manner.

The preformed heterodimer mechanism produces the signaling complex in a different manner [14, 15, 16, 17, 18]. Before interleukin-2 becomes involved in the process, the IL-2α receptors and IL-2β receptors must first find each other in the two-dimensional cell membrane and form a complex. This complex has been termed the high-affinity interleukin-2 receptor, having a K_d of $1x10^{-11}M$ [17]. Once the IL-2α/IL-2β heterodimer has been formed, interleukin-2 must diffuse through the bulk

solution and bind to the heterodimer in a ligand-surface association.

The area of controversy in regards to this mechanism is the question of whether the receptors are truly separate in the cellular membrane or if a heterodimer of both the IL-2 and the IL-2 exists as the receptor [14, 15, 16, 17, 18]. This recent experimental work purports to have shown that a heterodimeric receptor for IL-2 is the proper model, although the evidence presented there is still not conclusive. The problem with these studies is that they attempt to make use of equilibrium techniques to describe what is indeed a kinetics problem. It is the intent of this study to use theoretical computer-modeling of kinetics to determine which of these two proposed mechanisms is the one which best describes the formation of the interleukin-2 -receptor complex.

2 Introduction

2.1 General Description of the Model and Study

The study of the kinetics of biological systems has become a useful tool for understanding the actual interactions involved in such systems [14]. The present study uses theoretical kinetics to model the formation of IL2-IL2α complexes and IL2-IL2β complexes on the surface of the human T-cell.

Recently much work has been done on the interleukin-2 system [14, 15, 16, 17, 18]. Of particular interest is the question of the presence of preformed receptor heterodimers. Much of this work has supported the existence of such preformed

heterodimers but detailed theoretical kinetic results have not yet been provided.

It is the purpose of the present study to use the method of Waite [1] to model the kinetics of the interleukin-2 system. The diffusion-kinetics interactions of ligands with cell-membrane bound receptors, including the formation of ligand-receptor complexes which lead to signal transduction, are described by a set of differential equations which are obtained by combining the appropriate rate terms for each of the species in the model. There are analogous rate terms for free-ligand cell surface interactions and membrane-bound species interactions with parameters for each adjusted accordingly. The proposed species for this study are listed in Table 1.

This present study involves both a simple and a complex model of the diffusion-kinetics of the interleukin-2 system. The simple model is a preliminary step to the eventual theoretical diffusion-kinetics solution to the interleukin-2 preformed heterodimer problem. This model considers the interaction between interleukin-2 and the IL-2α receptor and the interaction between interleukin-2 and the IL-2β receptor but not the interactions between IL-2α receptors and IL-2β receptors.

The complex model is used to actually solve the interleukin-2 preformed heterodimer problem. It allows the IL-2α receptors and IL-2β receptors to interact and possibly form the heterodimer IL- 2α/IL-2β which can then either dissociate or bind interleukin-2 to form the signaling complex.

Ligands bound non-specifically to the cell surface (glycocalyx) are included in both models. Parameters such as diffusion coefficients, probabilities of binding, and

lifetimes of involved diffusing species are arrived at theoretically [2] or by fitting theoretical data empirically to actual experimental data.

2.2 Quantitative Aspects of the System

The system used in this study consists of a volume of solution, V, containing n_{cell} cells of radius R_{cell}. Each cell surface has n-sites of radius r with a diffusion coefficient D [1]. For the simple model these sites consist of species 2-11 as listed in Table 1A. For the complex model these sites consist of species 2-17 as listed in Tables 1A and 1B.

Each cell can be assigned varying initial numbers of species and varying probability factor, diffusion coefficients, and dissociation constants. The concentrations of all species involved in the system are more conveniently written in terms of number densities rather than molar concentrations as all calculations are based on the number of species per cell.

The surface number density (m^{-2}) of a particular species, β, is simply the number, n_β, of that particular species present divided by the surface area of the cell [1]

$$N_\beta = n_\beta / 4\pi R_{cell}^2 \tag{1}$$

In this model all of the β species are sites where specific binding can take place. These sites include species 2-17 as defined previously in Table 1.

The fraction of the cell surface occupied by these sites is [1]

$$f_\beta = N_\beta \pi r_\beta^2 \tag{2}$$

As shown by Waite [1], the non-specific binding sites on the glycocalyx of the cell do not have number densities. The fraction of cell surface available for non-specific binding is given by

$$f_g = 1 - \sum_\beta f_\beta \tag{3}$$

where the summation is over all of the possible binding sites, β, defined above [1].

Bulk free ligand particles are also present in this system. They are described in a similar manner as the surface bound species in that they have radius r_l and diffusion coefficient D_l [1]. The volume number density of ligands (m^{-3}) is

$$N_l = M_l N_A \cdot 1000 \tag{4}$$

where M_l is the molar concentration of ligand and N_A is Avogadro's number [1].

2.3 Dimensional Aspects of the Diffusion-Kinetics Model

Diffusional rate constants are based on classical kinetics with some important modifications. These differences are necessitated by the fact that the receptors and ligands involved in the theoretical kinetics model do not undergo strictly three dimensional interactions.

An encounter of two bodies in solution can be modeled by the following second order rate law [1]:

$$rate = k[A][B] \tag{5}$$

where k is the rate constant for the reaction in m^3s^{-1} and $[A]$ and $[B]$ are the concentrations of species A and B in m^{-3}, respectively.

A problem arises when this type of rate law is applied to a ligand-receptor interaction. This is because the ligand is in solution and has three degrees of freedom, but the receptor is solvated in the cellular membrane and has only two degrees of freedom. For the normal solution case, the second-order rate constant would be expected to have units of m^3s^{-1} as shown above.

Waite [1] has shown that if the rate of disappearance of a substrate is being measured, then the rate constant must be expressed in terms of m^2s^{-1} [10]. Similarly if the rate of disappearance of a membrane bound species is being measured, then the rate constant must be expressed in terms of m^3s^{-1} [1]. It is convenient then to define a conversion between these rate constants for surface species and those for solution-phase species. Waite [1] has defined this conversion as

$$k_{3D} = Ck_{2D} \tag{6}$$

where $C = 4\pi R_{cell}^2 n_{cell}/V$, which is the ratio of the total surface area of all the cells in the system to the total volume of the system.

3 Derivation of Ligand-Surface Kinetic Terms

3.1 Ligand-Surface Associations

The total flux J of initial encounters of free ligand with a cell surface of radius R_{cell} is given by [1]

$$J_{l-cell} = 4\pi D_l R_{cell} N_l \tag{7}$$

The total rate of disappearance of free ligand due to encounter with the cell surface is [1]

$$rate = k_{l-cell}^{assoc.} N_l \tag{8}$$

where

$$k_{l-cell}^{assoc.} = 4\pi n_{cell} D_l R_{cell} / V \tag{9}$$

Upon initial encounter of free ligand, l, and a cell receptor site, β, one of three events is possible. The ligand can bind to the receptor site with probability $P_{\beta-l}$, the ligand can escape to the bulk medium and become free once again with probability $(1 - P_{\beta-l})\, P_{esc}$, or the ligand can rebound from the receptor site and enter a non-free state with probability $(1 - P_{\beta-l})\,(1 - P_{esc})$. These interactions are represented by the following kinetic steps [1]:

$$l+\beta \rightarrow \left\{ \begin{array}{c} l-\beta \\ l \cdots \beta \\ l+\beta \end{array} \right\} \tag{10}$$

The term P_{esc} is the probability that a ligand can diffuse from the cell surface into the bulk without subsequent re-encounters with the cell surface and is equal to $r_l/(r_{cell}+r_l)$ [1]. Each of these probability factors modifies the rate constant for a given type of interaction.

The explicit term of the total rate of appearance of species resulting from bulk to surface associations is the total flux of free ligand at the cell multiplied by the fraction of the surface area occupied by receptor site [1]:

$$rate = Jf_\beta/V = 4\pi^2 n_{cell} D_l R_{cell} r_\beta N_l N_\beta / V \tag{11}$$

The modification of this rate law by the appropriate probability factors gives the rate of appearance of species $l-\beta$ and $l \cdots \beta$. No rate term is needed for the case where the result is $l+\beta$ because there has been no net change in the numbers of β or l present.

It would appear that as a species formed it could itself become a receptor site and eventually lead to the introduction of many very complex species into the model.

The simplifications of these species take the general form

$$\begin{aligned}
(\beta - l) - l &\approx \beta - l \quad and \quad g - l \\
(\beta \cdots l) - l &\approx \beta - l \quad and \quad g \cdots l \\
(\beta - l) \cdots l &\approx \beta - l \quad and \quad g \cdots l \\
(\beta \cdots l) \cdots l &\approx \beta \cdots l \quad and \quad g \cdots l
\end{aligned} \tag{12}$$

3.2 Ligand-Surface Dissociations

All bound species eventually undergo dissociation by first-order kinetics with rate constants designated $k_{\beta-l}$. The rate law for such dissociations is

$$rate = k_{\beta-l}[N_{\beta-l}] \tag{13}$$

Two events are possible upon dissociation: the ligand can remain associated with the cell surface through rebounding interactions with probability $1 - P_{esc}$ or the ligand can escape to the bulk medium without subsequent re-encounters with the cell surface with probability P_{esc}. The dissociation of bound species can be represented by the following elementary kinetic steps [1]:

$$l - \beta \rightarrow \left\{ \begin{array}{c} l \cdots \beta \\ \\ l + \beta \end{array} \right\} \tag{14}$$

The first-order dissociation rate constant of a bound complex is related to the half-life ,$\tau_{1/2}$, of the bound complex as shown below

$$\tau_{1/2} = \frac{\ln 2}{k_{\beta-l}} \tag{15}$$

These dissociation rate constants are modified by the appropriate probability factor depending on what type of dissociative event is occurring.

3.3 Ligand-Surface Rebounding Interactions

Localized free ligands which are loosely associated with the cell surface are all possible species $\beta \cdots l$. These species undergo re-encounters with the cell surface with a total average frequency of [1]

$$\nu_{tot} = 2(1 - \ln 2)D_l/r_l^2 \tag{16}$$

Re-encounters at the surface will occur either at the site of origin, β, or some new location on the cell surface, α. For simplicity, rebounding encounters at the site of origin are assumed to have the same probability parameters as if the ligand had been of the free type [1]. The possible outcomes of rebounding associations both at the site of origin, β, or new cell surface sites, α, are represented by the following elementary kinetic steps [1]

$$\beta \cdots l \rightarrow \left\{ \begin{array}{c} \beta - l \\ \beta \cdots l \\ \beta + l \end{array} \right\} \tag{17}$$

$$\beta \cdots l + \alpha \rightarrow \left\{ \begin{array}{c} \beta + \alpha - l \\ \beta + \alpha \cdots l \\ \beta + \alpha + l \end{array} \right\} \tag{18}$$

The simplifications of complex species described above are invoked here to avoid introducing unnecessary complex species into the model.

The total re-encounter frequency, described above, includes all possible re-encounter sites. This can be divided into the frequency of re-encounter at the site of origin, ν_β, and the frequency of re-encounter at all other surface sites, ν_{res} [1]. This frequency of re-encounter at the site of origin is given by

$$\nu_\beta = \frac{D_l}{r_l^2} \sum_{n=0}^{\infty} \frac{(2n)!}{(n+1)!(n+1)!2^{2n+1}} \left[1 - \exp\left(\frac{-r_\beta^2}{4(n+1)r_l^2} \right) \right] \tag{19}$$

and the frequency of re-encounters beyond the site of origin is given by

$$\nu_{res} = \nu_{tot} - \nu_\beta \tag{20}$$

These frequency terms become the rate constants for these rebounding interactions.

4 Derivation of Membrane-Bound Diffusion-Kinetics Terms

4.1 General

In general, all of the bulk to surface terms derived above can be applied to the case of membrane bound interactions. In this case, however, initial encounter rates, re-

encounter frequencies, and escape probabilities are all based on results obtained from the two-dimensional diffusion equation [1]. The membrane bound steps also need only consider interactions between species that may successfully bind, since it is only these interactions which lead to the formation of new species, whereas all bulk to surface interactions give rise to new species [1].

4.2 Membrane-Bound Associations

Consider the free surface species ω and γ ,diffusing randomly in the two-dimensional matrix of the cell membrane. Each species has diffusion coefficient, D_ω or D_γ, and radius, r_ω or r_γ. The term *bulk free* represents species that are not part of an interacting pair and are beyond the boundary of interactions, L [1].

The total rate of membrane bound encounters between species ω and γ is given by [1]

$$rate = k_{\omega-\gamma}[N_\omega][N_\gamma] \tag{21}$$

with a rate constant of [1]

$$k_{\omega-\gamma} = 2\pi(D_\gamma + D_\omega)/\ln\left(\frac{L}{r_\gamma + r_\omega}\right) \tag{22}$$

In this case, L is simply the average distance between particles on the cell surface [1].

These encounters can be represented by the following elementary kinetic steps [1]

$$\omega + \gamma \rightarrow \left\{ \begin{array}{c} \omega - \gamma \\ \omega \cdots \gamma \\ \omega + \gamma \end{array} \right\} \tag{23}$$

Analogous to the ligand surface case, the formation of complex $\omega - \gamma$ is governed by the probability factor $P_{\omega-\gamma}$, the formation of the species $\omega \cdots \gamma$ is governed by the probability factor $(1 - P_{esc})(1 - P_{\omega-\gamma})$, and the return of both particles to the bulk after encounter is represented by $(1 - P_{\omega-\gamma})P_{esc}$ [1]. In these terms $P_{\omega-\gamma}$ is the probability of binding per encounter and P_{esc} is the probability of escape to the bulk state and is given by [1]

$$P_{esc} = \ln 2 / \ln \left(\frac{L}{r_\omega + r_\gamma} \right) \tag{24}$$

As in the ligand surface case, a newly formed bound species may also serve as a free surface species ω or γ. Simplifications are made in this case, analogous to those preformed in the ligand surface case, in order to eliminate highly complex species from the model.

4.3 Membrane-Bound Dissociations

Complexes formed from bound surface species also undergo dissociation by first-order kinetics. Each surface dissociation occurs according to the rate law where $k_{\omega-\gamma}$ is the rate constant defined by Waite [1]. The rate of this dissociation is given by

$$rate = k_{dissoc.}[N_{\omega-\gamma}] \tag{25}$$

where $k_{dissoc.}$ is the first-order dissociation rate constant.

Two outcomes are possible upon surface dissociation: the species ω and γ can re-encounter one another to form the species $\omega \cdots \gamma$ or the species ω and γ can recede beyond the distance L, becoming free surface species without undergoing subsequent associative re-encounters. Formation of the species $\omega \cdots \gamma$ is governed by the probability parameter $(1 - P_{esc})$ and formation of free surface species is governed by the probability parameter P_{esc} [1]. The elementary kinetic steps representing such dissociations are [1]:

$$\omega - \gamma \rightarrow \left\{ \begin{array}{c} \omega \cdots \gamma \\ \\ \omega + \gamma \end{array} \right\} \tag{26}$$

4.4 Membrane-Bound Rebounding Associations

The total frequency of re-encounter for surface species $\omega \cdots \gamma$ is given by [1]

$$f_{2D}^{reb} = 0.460 \left(\frac{D_\gamma + D_\omega}{(r_\gamma + r_\omega)^2} \right) \tag{27}$$

The elementary kinetic steps representing these rebounding interactions are [1]

$$\omega \cdots \beta \rightarrow \left\{ \begin{array}{c} \omega - \beta \\ \omega \cdots \beta \\ \omega + \beta \end{array} \right\} \tag{28}$$

Rebounding encounters leading to bound species $\omega - \gamma$ are governed by the probability term $P_{\omega-\gamma}$, rebounding encounters leading to the formation of rebounding species $\omega \cdots \gamma$ are governed by the probability parameter $(1 - P_{\omega-\gamma})(1 - P_{esc})$, and rebounding encounters leading to the production of free surface species are governed by the probability parameter $(1 - P_{\omega-\gamma}) P_{esc}$ [1].

5 Method of Writing Rate Laws

Rate laws governing the time rate of change of bulk ligand and possible surface species were written using the appropriate bulk to surface kinetic terms and membrane-diffusion kinetic terms. These terms where then translated into FORTRAN code. The rate law for any given species is formed by summing all of the rate law terms for the mechanistic steps that contribute to the appearance or disappearance of that particular species.

A brief example of this is provided by examining rate terms governing the time rate of change of the species resulting from the bulk to surface association of a ligand molecule and a cell surface receptor site, β.

- Mechanistic Step for Ligand-Surface Association [1]

$$l + \beta \rightarrow \left\{ \begin{array}{l} a)\ l - \beta \\ b)\ l \cdots \beta \\ c)\ l + \beta \end{array} \right\} \tag{29}$$

It is of interest to note that no rate terms are needed for step c because there is no net change in the number of free ligand or receptor site β.

- Rate Terms for Ligand-Surface Association [1]

The following terms govern the appearance of the products indicated in the steps given above.

$$\begin{array}{ll} a) & rate = P_{i-l} J_{i-cell} f_i / VC \\ b) & rate = (1 - P_{i-l})(1 - P_{esc}) J_{i-cell} f_i / VC \end{array} \tag{30}$$

Identical, negative terms are written for the disappearance of the reactants, except that the conversion from three dimensions to two dimensions ($C = 4R_{cell}^2 n_{cell}/V$) is not needed in this case for the disappearance of the ligand.

- Rate Terms Translated into FORTRAN

As shown above, the rate term for this case is the total flux of encounters between bulk-ligand and a cell surface (J) multiplied by the appropriate probability factor divided by the total volume of the system and the three dimensional to two dimensional conversion factor. The value of the flux was used frequently in the FORTRAN code and hence labelled as a constant variable, rl.

a) FORTRAN term = +rl*frac(2,y)*pil/c

b) FORTRAN term = +rl*frac(2,y)*(1-pil)*(1-pesc)/c

The term frac(2,y) is simply the fraction of the cell surface covered by the i receptor. Corresponding numbers are assigned to other species in the model as shown in Table 1. P_{i-l} is the probability of association for the bulk to surface interaction of free ligand and an i receptor and P_{esc} is the probability of escape from the cell surface without re-encounter. Experimentally important parameters are defined in Table 2.

The resulting FORTRAN program is run in order to generate the kinetic data. The coupled differential equations are solved using the DIVPAG subroutine which is based on the method of Gear. The number of differential equations needed is equal to the number of species present in the model, eleven for the simple model and seventeen for the complex model. The data is analyzed using the ttro spreadsheet package QUATTRO, version 4.0.

6 Experimental Kinetic Runs Leading to the Solution of the Preformed Heterodimer Problem

6.1 The Simple Model with Identical Receptors

Kinetic runs were performed using the eleven species given in Table 1A. It is of interest to note that these species include no possible interactions between the two types of receptors. This is to insure that the system is well behaved with no negative

concentration values and a constant sum of the numbers of both i and j ligands between all species where these ligands are involved.

Two types of runs were carried out in order to elucidate the behavior of two types of natural intercellular signaling: autocrine growth and paracrine growth. The autocrine growth runs allowed no initial free bulk ligand and 100000 initial non-specifically bound ligands in addition to 50000 each of i and j receptors. The majority of the runs describe paracrine growth because this is the major mechanism of intercellular signaling. These runs had 50000 each of i and j receptors and a bulk free ligand concentration of $1x10^{-9}M$.

6.2 The Complex Model with Identical Receptors

The complexity of the system was increased with the addition of i and j receptor interactions. This change gave rise to the additional species presented in Table 1B. The addition of these species was important in showing whether or not the system continued to be well-behaved as the types of interactions were made increasingly complicated. As before, 'well- behaved' is defined to mean no negative numbers of species and a constant sum of i and j receptors regardless of their form, i.e. complexed or unbound, bound to a particular receptor, etc.

Three types of kinetic runs were investigated in order to elucidate the behavior of the system for each type of intercellular signaling. As before both autocrine and paracrine growth were studied, with the addition of a realistic autocrine and paracrine

growth system in which free bulk ligand and non-specifically bound ligand is provided at the beginning of the kinetic run. The autocrine runs have 3000 non-specifically bound ligand and 1000 each of i and j receptors. The paracrine runs have an initial ligand concentration of $1x10^{-9}M$ and 1000 each of i and j receptors. The combination runs have initial concentration of ligand of $1x10^{-9}M$, 1000 each of i and j receptors, and 3000 non-specifically bound ligand.

6.3 The Complex Model with Non-identical Receptors

The actual interleukin-2 system is modeled using differing receptors. The IL-2α receptor, represented in the model by the i receptor, has a higher binding affinity for interleukin-2 than the IL-2β receptor, represented in the model by the j receptor.

As in the complex model with identical receptors, autocrine growth, paracrine growth, and the combination of the two are modeled using the same concentrations of bulk ligand, non-specifically bound ligand, and i and j receptors as described for the case of the complex model with identical receptors. It was these runs which provided the theoretical kinetics solution to the preformed heterodimer problem.

7 Results and Discussion

7.1 The Simple Model

7.1.1 Default Data

The first step in understanding the complete paracrine growth mechanism was to obtain data showing the time rate of change of the amounts of the species of interest under the initial conditions in the default data set. Representative ligand-receptor association curves for this data set are given in Figure 1. This run provided the baseline data for comparison to other sets of data obtained using modified parameters, which will ultimately be the tool used to elucidate the overall mechanism.

7.1.2 Change of Cell Radius

At all times the larger cell ($R_{cell} = 1x10^{-5}m$) has a greater number of non-specifically bound ligands, due to the fact that its surface area is 100 times larger than the default cell ($R_{cell} = 1x10^{-6}m$) (Figure 1a). Initially, the number of complexes of either type is greater for the default cell. This is because the surface density of receptors is higher in the default cell, making it easier for free ligand to "find" an i or j receptor. Figure 1c shows that at 3 milliseconds, the larger cell begins to have more i-l complexes than the default cell. This is counter to the explanation offered above due to the surface area change and therefore another mechanism must predominate: membrane-bound association. There is more non-specifically bound ligand on the surface of

the larger cell due to its larger surface area, providing a greater surface density of non-specifically bound ligand in the larger cell. This makes it easier for the surface bound i and j receptors to associate with membrane bound ligand in the larger cell. The point in time where the default cell begins to lag behind the larger cell in the number of bound-receptor ligand complexes is the point in time where the mechanism switches from predominantly bulk to surface associations to predominantly membrane diffusion associations.

The predominance of the membrane-bound association is further shown by comparison of association rate constants for the complex i-l for cells having radii of 1 micron and 10 microns (Figure 1b). The rate constants are determined using the method of initial slopes and are given and compared to values obtained by Landgraf, et al., in Table 3 [14].

7.1.3 Elimination of Ligand-Surface Associations for I-L

The only way to form the bound receptor-ligand complex, i-l, was through membrane diffusion associations. The ligand was allowed to form bound receptor-ligand complexes with the j receptor via both bulk to surface association and cell membrane association.

The ligand-receptor curve for this case is shown in Figure 2a. The difference between the numbers of i-l in the case where ligand surface interactions have been eliminated and the default case becomes progressively less significant with time. At all times the number of i-l formed by both bulk to surface association and membrane-

diffusion association is greater than the number of i-l formed by membrane-diffusion association alone. At longer times, the number of i-l complexes formed when ligand-surface associations have been eliminated approaches the number of i-l complexes formed in the default case.

It is of interest to note that the rate of formation of j-l complexes when IL-2-receptor ligand surface associations have been removed is greater than the rates of formation of i-l and j-l complexes under the default conditions. The rate constants are determined by the method of initial slopes (Figures 2b,c) The effective number of j-l complexes formed increases in this case because the j receptor does not have to compete with the i receptor for free ligand in bulk to surface associations.

7.1.4 Elimination of Membrane-Bound Associations for I-L

In this case the only way to form the bound receptor-ligand complex, i-l, is via a bulk to surface association mechanism. As in the trials where ligand-surface interactions were eliminated for the receptor and interleukin-2, the ligand was allowed to complex with the j receptor via both mechanisms.

The differences between the number of i-l in the case where membrane-bound associations have been eliminated and the default data becomes increasingly significant with time (Figure 2a). At larger times this difference increases to the point where the i-l complexes formed in the default case vastly outnumber the i-l complexes due to the fact that the i-l complex can be formed via both mechanisms in the default case and the i-l complex can be formed by the bulk to surface mechanism alone in

the other case.

It is interesting to note that the rate of formation of j-l complexes formed when membrane-bound associations have been eliminated is greater than the rate of formation of i-l and j-l complexes formed under default conditions. This is because the j receptor does not have to compete with the i receptor for ligand in membrane-diffusion associations, which is not allowed experimentally for the i receptor. The rate constants were determined by the method of initial slopes as shown in Figures 2 b and c.

7.1.5 Elimination of Ligand-Surface Associations for I-L and Change of the Cell Radius

As in the case when $R_{cell} = 1x10^{-6}m$ and ligand-surface associations have been eliminated (Figure 2a), the production of i- l complex initially lags behind the production of i-l complex in the default case (Figure 3a) when $R_{cell} = 1x10^{-5}m$ and ligand-surface associations have been eliminated. At longer times the production of i-l complex for this case surpasses that of the default case. The larger cell has more non-specifically bound ligand that can be converted to bound-receptor ligand complex by membrane-bound associations, which are the only way that the complex i-l may form. The association rate constants for this case are calculated using the method of initial slopes Figure 3b and are given in Table 3.

7.1.6 Elimination of Membrane-Bound Associations and Change of the Cell Radius

As in the case when $R_{cell} = 1x10^{-6}m$ and membrane bound associations have been eliminated (Figure 2a), the rate of production of i-l complex for this case initially matches the rate of production of i-l complex for the default case. At long times, however, the production of i-l complex in this case cannot keep pace with the production of i-l in the default case (Figure 3a).

The larger cell size makes it harder for the ligand to find the receptors on the cell surface since the overall number density of the receptors is decreased by a factor of 100. Ligand-surface associations are the only way to form the complex i-l and thus the fact that the larger cell has more non-specifically bound ligand is immaterial. Thus, the rate of i-l complex production for the case of larger cell elimination of membrane-bound interactions is less than the rate of i-l complex production in the default case, as shown by the rate constants in Table 3. These rate constants were calculated using the method of initial slopes as shown in Figure 3c.

7.1.7 Relationship Between Non-specifically Bound Ligand and Receptor-Ligand Complexes

The ligand receptor association curves for these trials are given in Figure 4. When the bulk to surface mechanism is predominant, the numbers of non-specifically bound ligands and ligand-receptor complex behave independently. At longer times the dif-

fusion kinetics mechanism takes predominance and the number of non-specifically bound ligands stays relatively constant as the number of bound i receptor-ligand continues to grow because the non-specifically bound ligands collide with unbound receptors to form bound receptor-ligand complexes.

As the number of bound receptor-ligand complexes approaches its maximum value (50003 for these trials) the number of non-specifically bound ligands increases dramatically. There are progressively fewer and fewer free receptors of either type to interact with the non-specifically bound ligand because most of them have been used up in receptor-ligand complexes. The only place that a ligand can bind to the cell is the cell membrane itself. The result is the rapid increase in the number of non-specifically bound ligand-cell membrane complexes. This result is even more exaggerated in a system containing cells with radii of $1x10^{-5}m$. Even more of the cell surface is available for the non- specific binding of ligand to the cell membrane after all of the free i and j receptors have been consumed.

7.1.8 Elimination of Non-specifically Bound Ligand

These studies were carried out with cells of radius $1x10^{-6}m$ and $1x10^{-5}m$ in order to elucidate the relationship between non-specifically bound ligand and receptor-ligand complexes shown in Figure 4 and discussed above. In both cases, when ligand-surface interactions have been eliminated (Figures 5 a,b) the number of i-l and j-l receptor-ligand complexes reached an equilibrium number of 2.50 before receding back to zero because of dissociation. The initial amount of non-specifically bound ligand

was quickly used by the i and j receptors in the formation of i-l and j-l complexes. Dissociation of these complexes gave bulk free ligand instead of non-specifically bound ligand because the probability of formation of non-specifically bound ligand was set to 0.

When membrane-bound associations were eliminated (Figures 5a,b) the number of receptor-ligand complexes almost reached the maximum value of 50003 for these experimental conditions. The complexes i-l and j-l are produced by solely by the ligand-surface association mechanism. Thus non-specifically bound ligand is necessary for the formation of bound receptor-ligand complexes and has no effect on the ligand-surface mechanism.

7.1.9 Half-Lives of I-L and G-L Complexes

The half-life of the i-l bound receptor ligand complex was obtained by setting eliminating both ligand-surface and membrane-bound associations in the model. Therefore once a complex had dissociated there was no way for re-association. The first order rate constants of dissociation were obtained from the first order plot shown in Figure 6 for non-specifically bound ligand and the complex i-l for cells with a radius of 1 micron and 10 microns. These rate constants and half-lives are listed in Table 3 and compare favorably to actual experimental work [14].

7.1.10 Modification of the Diffusion Coefficient of the Ligand

In the case where $D_l = 1x10^{-5}m^2s^{-1}$, the diffusion constant of the ligand is increased to the point that the rate of formation of bound-receptor ligand complexes is greater than that seen in the default data where $D_l = 1x10^{-10}m^2s^{-1}$. The membrane-diffusion mechanism predominates and produces bound-receptor ligand complex more rapidly because the ligand is better able to move in the two- dimensional matrix of the cell membrane (Figure 7a).

When $D_l = 1x10^{-15}m^2s^{-1}$, the diffusion constant of the ligand is decreased to the point that it moves much slower while solvated in the cellular membrane. This makes it harder for receptors and non- specifically bound ligand to associate. The great increase in rate of complex production seen in the default data from membrane-diffusion associations is absent. The bulk to surface mechanism predominates and cannot produce large numbers of bound complexes as quickly as the membrane-diffusion mechanism (Figure 7a). Changing the cell radius to 10 microns gave similar results in both cases as shown by Figure 7b.

7.1.11 Study of Autocrine Growth Via Elimination of Free Ligand and Ligand-Surface Associations

The general behavior exhibited when autocrine growth is the growth mechanism for the system is that the complex i-l forms at the same rate whether or not ligand-surface associations are included in the model. This is shown by the ligand-receptor

association curves given in Figure 8. The insignificant difference between the number of i-l complex in the default autocrine case and in the case where ligand-surface interactions have been removed from the model shows that the primary mechanism for autocrine growth is membrane-diffusion associations. Bulk to surface associations are insignificant in autocrine growth because little interleukin-2 manages to escape the cell surface and become the bulk free ligand necessary to give rise to ligand-surface associations.

7.2 The Complex Model with Identical Receptors

7.2.1 Experimental Conditions

All runs for the complex model with identical receptors were conducted with 1000 of each type of receptor present on the cell surface. The autocrine growth runs had 3000 non-specifically bound ligand present on the cell surface and there was no bulk free ligand present in the system. The paracrine growth runs had no non-specifically bound ligand present initially and a bulk free ligand concentration of $1x10^{-9}M$. The combined autocrine-paracrine growth mechanism, which most closely simulates the actual interleukin-2 system, had 3000 non-specifically bound ligand present on the cell surface and an initial bulk free ligand concentration of $1x10^{-9}M$. Each receptor has identical probability parameters so that associations for each take place at the same rate.

7.2.2 Autocrine Growth Case

Figure 9 shows the ligand-receptor association curves for autocrine growth. In the default data case the signaling complex, represented by (i-j)-l, reaches an equilibrium value of 320 complexes at a time of 10 milliseconds. Other important species include the i-l and j-l complexes, which reach an equilibrium value of 620 complexes at 5 milliseconds, and the preformed heterodimer which reaches a maximum of 90 complexes at 1 millisecond. This plot shows that the complex i-l is formed faster than the preformed heterodimer i-j.

In the case where ligand-receptor interactions are eliminated ($P_{i-l} = 0, P_{j-l} = 0, P_{2i-l} = 0, P_{2j-l} = 0$) a completely different set of ligand- receptor curves are obtained. The complexes i-l and j-l are not present during the course of the run because the probabilities of association either by ligand-surface associations or membrane-bound associations are 0. The equilibrium for the (i-j)-l signaling complex has changed with respect to the default data case. The equilibrium number of the signaling complex achieved is much greater than that of the default data case and reaches a maximum of 990 complexes and an average equilibrium value of 975 complexes. The equilibrium value is achieved at 0.5 seconds, much later than the default data case.

The complex i-j in this case reaches a greater maximum that in the default data case because there are no i-l or j-l complexes being formed. Thus all of the i and j receptors are available for preformed heterodimer formation.

The case when preformed heterodimer formation is eliminated ($P_{i-j} = 0$) shows

behavior that is similar to the default data set. The signaling complex (i-j)-l reaches an equilibrium value of 320 complexes at a time of 10 milliseconds, as was the case for the default data set. The i-l complex ligand-receptor association curve for this case also matches that of the default data case.

7.2.3 Autocrine and Paracrine Growth Case

Figure 10 shows the ligand-receptor association curves for the autocrine and paracrine growth system. This most closely models the actual behavior of the immune system where cells receive signals via both mechanisms. Here the behavior of the default case closely matches that of the autocrine growth only system. The (i- j)-l signaling complex reached an equilibrium value of 320 complexes at 10 milliseconds and the i-l and j-l complexes reached an equilibrium value of 620 complexes at 9 milliseconds. As was the case with the autocrine growth only runs, only a small number of the preformed heterodimer (i-j) was present and quickly disappeared.

The case where ligand-receptor associations were eliminated shows an equilibrium value of 975 complexes reached at 0.5 seconds. This equilibrium is much larger than for the default case because there are no i-l or j-l complexes present in the system. All of the receptors first form the i-j heterodimer and then bind bulk free ligand to produce the signaling complex.

The case where preformed heterodimers are eliminated behaved in a similar fashion to the default case. The complex (i-j)-l reached an equilibrium value of 320 complexes at 10 milliseconds and the i-l and j-l complexes reached equilibrium values of 680

complexes in each case at a time of 9 milliseconds. The number of i-l and j-l formed is slightly higher than in the default case because there are no i and j receptors in the form of the preformed heterodimer i-j.

7.2.4 Paracrine Growth Case

Figure 11 shows the case for a system that allows formation of ligand-receptor complexes through the paracrine growth mechanism only. The paracrine growth only case shows behavior that differed greatly from the previously described cases. The default paracrine growth case shows a large number of preformed heterodimers present before the complex i-j-l was produced to any appreciable amounts. The complexes i-l and j-l are not present to any great extent in this case.

The case where ligand-receptor associations were eliminated shows behavior that more closely matches the two previously mentioned cases. The complex i-j-l reached an equilibrium value of 975 complexes at a time of 1 seconds closely matching the equilibrium number and time of the autocrine only and autocrine/paracrine cases. The main difference, however, is the presence of a great number of the preformed heterodimer at 60 milliseconds. The maximum value reached is just over 900 complexes which quickly recedes as the complex i-j-l is produced.

The case where the preformed heterodimer formation is eliminated shows unusual results in that the complex i-j-l is produced without any appreciable numbers of i-l or j-l complexes being present, which were present in the autocrine and autocrine/paracrine systems.

7.2.5 Discussion of Results for the Complex Model with Identical Receptors

The autocrine and autocrine/paracrine systems showed almost identical behavior and will be treated together. It is of interest to note that in both of these systems, the case where preformed heterodimers were removed from the model most closely resembled the default data case where all models were present, both equilibrium numbers of complexes formed and the time at which equilibrium was achieved. For these systems then, the formation of the signaling complex i-j-l must occur via the affinity conversion model. The case where ligand-surface interactions have been eliminated shows that indeed the signaling complex (i-j)-l may be formed by the preformed heterodimer model. However, in this case the equilibrium number of i-j-l is reached at a later time than in the autocrine and autocrine/paracrine cases.

This allows the following generalizations to be made about the nature of the system when applied to the interleukin-2 problem. The complexes i-l and j-l must be formed faster than the preformed heterodimer. This is shown by the fact that the equilibrium number of complexes is obtained at 10 milliseconds for the default and no preformed heterodimer cases and at 0.5 seconds for the case where ligand-receptor interactions have been eliminated. The preformed heterodimer model is suppressed in the default case because the i and j receptors bind ligand to become the complexes i-l and j-l much faster than they bind each other to become the preformed heterodimer. These complexes then diffuse about randomly until they find the other type of receptor and

form the signaling complex i-j-l.

The paracrine growth model is unique in that no non-specifically bound ligand is initially present on the surface of the cells. The default case shows many preformed heterodimers before the production of the signaling complex because the diffusion of the i and j receptors leads only to the formation of preformed heterodimer. The complexes i-l and j-l are produced only by the ligand-surface mechanism, which was shown in the simple model to lead to a small equilibrium number of these complexes when compared to the membrane-bound mechanism (Figure 3a). The results of the paracrine only case reinforce the concept that the membrane-bound interactions are the predominant interactions, even though they take place over longer time periods than ligand-surface interactions. Thus the autocrine/paracrine model shows the results obtained for the autocrine only model, where ligand surface interactions are not present, and not the paracrine only model, where these ligand surface interactions predominate.

7.2.6 Comparison of Kinetic Results to Actual Experimental Values

Dissociation rate constants were measured for the species i-l, g-l, i-j, and (i-j)-l and are compared to experimentally obtained values [14] in Table 1. The first-order dissociation plots for these species are given in Figure 12. The association rate constant for the species (i-j)-l obtained from the default data run is compared to an experimentally obtained value [14] in Table 1.

7.3 The Complex Model with Non-Identical Receptors

7.3.1 Experimental Conditions

All runs were conducted in a manner similar to that for the case of identical receptors in that autocrine only, paracrine only, and autocrine/paracrine systems were examined. The difference was that the probability parameters for the two receptors were changed so that the interleukin-2 ligand bound to the IL-2α receptor with a higher probability than it bound to the IL-2β receptor.

7.3.2 Autocrine Growth Case

Figure 13 shows the ligand-receptor association curves for the autocrine growth only case. For the default case, it is of interest to note that the complex i-l is formed faster than the complex j-l and that both of these species reach an equilibrium value of 560 complexes at times of 1 and 5 milliseconds respectively. The complex (i-j)-l reaches an equilibrium value of 380 complexes at a time of 10 milliseconds.

The case where ligand-receptor associations have been eliminated shows an equilibrium value of the number of (i-j)-l complexes of 980 reached at a time of 0.5 seconds. This is because no i and j receptors are used up in the form of the complexes i-l or j-l, thus all available i and j receptors can be used to form the preformed heterodimer i-j.

The case where preformed heterodimers have been eliminated shows behavior that resembles that of the default case. The complex i-l is formed faster than the complex

j-l and both of these complexes reach equilibrium at 1 milliseconds and 5 milliseconds respectively. The numbers reached (625) in both cases is greater than the default case because no i and j receptors are in the form of the preformed heterodimer.

7.3.3 Autocrine and Paracrine Growth Case

The behavior of the autocrine/paracrine system is shown in the ligand-receptor association curves given in Figure 14. These ligand-receptor curves closely resemble those obtained in the autocrine only case.

The default data case shows that the i-l complex is produced faster than the j-l complex. Both complexes reach an equilibrium value of 560 complexes at times of 1 and 5 milliseconds, respectively. The complex (i-j)-l reaches an equilibrium value of 380 complexes at 10 milliseconds.

The case were ligand-receptor associations have been eliminated show the large number of (i-j)-l complexes characteristic of this case, with an equilibrium number of 980 complexes being reached at 0.5 seconds. The increased number of complexes can again be attributed to the fact that no i or j receptors are used up as either the i-l complex or the j-l complex. Elimination of the preformed heterodimer produces behavior that resembles that of the default case. The production of the complex i-l occurs faster than the production of j-l. Both complexes reach an equilibrium value of 625 complexes at times of 1 and 5 milliseconds, respectively. The increased number of i-l and j-l complexes can again be attributed to the absence of the preformed heterodimer, providing more free i and j receptors.

7.3.4 Paracrine Growth Case

The ligand-receptor association curves for these trials are shown in Figure 15. The paracrine growth only case showed behavior that differed greatly from the previously described cases. The default paracrine growth case showed a large number of preformed heterodimers present before the complex i-j-l was produced to any appreciable amounts. The complexes i-l and j-l were not present to any great extent in this case, except at long times where dissociation of the complex (i-j)-l gave rise to these species.

The case where ligand-receptor associations were eliminated shows behavior that more closely matches the two previously mentioned cases. The complex i-j-l reached an equilibrium value of 975 complexes at a time of 1 seconds closely matching the equilibrium number and time of the autocrine only and autocrine/paracrine cases. The main difference, however, the presence of the maximum number of the preformed heterodimer at 60 milliseconds. The maximum value reached was just over 900 complexes. This number of preformed heterodimer was quickly reduced as the complex i-j-l was produced.

The case where the preformed heterodimer formation is eliminated shows unusual results in that the complex i-j-l is produced without any appreciable numbers of i-l or j-l complexes being present, which were present in large numbers in the autocrine only and autocrine/paracrine systems. Here the complexes i-l and j-l are only present at long times due to the dissociation of (i-j)-l.

7.3.5 Discussion of Results for the Complex Model with Non- Identical Receptors

The results for the complex model with non-identical receptors closely resemble the results obtained for the complex model with identical receptors. The autocrine and autocrine/paracrine systems both behaved very similarly and will be examined together. In these cases the affinity conversion model is again preferred over the preformed heterodimer models. This is shown by the fact that the system behaved the same in both the default case and the case where preformed heterodimers had been eliminated. In these cases the complex (i-j)-l was formed by 10 milliseconds compared to 0.5 seconds for the case where ligand-receptor associations had been eliminated. The formation of the complexes i-l and j-l is more rapid than the formation of the preformed heterodimer and thus the complex i-j-l is produced by the affinity conversion mechanism before it can be produced by the preformed heterodimer mechanism.

As was the case for the complex model with non-identical receptors, the paracrine growth model is unique in that no non-specifically bound ligand is initially present on the surface of the cells. The default case shows many preformed heterodimers before the production of the signaling complex because the diffusion of the i and j receptors leads only to the formation of preformed heterodimer. A small number of the complexes i-l and j-l are present because these complexes are formed ligand-surface associations only. As shown in the simple model, this leads to a small equilibrium number of these complexes when compared to the membrane-bound mechanism (Fig-

ure 3a).

The autocrine/paracrine model shows the results obtained for the autocrine only model, where ligand surface interactions are not present, and not the paracrine only model, where these ligand surface interactions predominate. This again shows that the membrane-bound diffusion interactions are the most significant interactions at long times.

8 Conclusion

The effectiveness of the application of a diffusion-kinetics system to ligand-receptor systems according to the method of Waite [1] has been demonstrated. The simple model has been used to describe the nature of these ligand-receptor interactions and prove the validity of theoretical results through comparison with actual experimentally obtained values. The complex model has been used to show that the affinity conversion model is the preferred mechanism for the formation of the interleukin-2 signaling complex according to theoretical diffusion kinetics. The theoretically obtained rate constants and half-lives given in Table 3 differ somewhat from experimentally obtained values [14] indicating that better estimates of parameters such as diffusion coefficients and radii are needed before the model simulates the behavior of the interleukin-2 system with complete accuracy.

FIGURE LEGENDS

FIGURE 1. Ligand - receptor association curves. The association curves for the IL-2-α receptor complex (shaded box for $r = 1x10^{-6}m$ and + for $r = 1x10^{-5}m$) and non-specifically bound ligand (* for $r = 1x10^{-6}m$ and empty box for $r = 1x10^{-5}m$): A. The association curves used to determine the association rate constants (listed in Table 3) for the IL-2-α receptor complex (shaded box for $r = 1x10^{-6}m$ and + for $r = 1x10^{-5}m$): B. The association curves for the binding of IL-2 by the α receptor showing switch from the predominance of bulk to surface associations to the predominance of membrane-bound diffusional associations at 3.0 msec: C. The association rate constants for the binding of IL-2 by the α receptor are determined from the initial slope as shown by Landgraf, et al. [14].

FIGURE 2. Ligand - receptor association curves. The association of IL-2 and α receptors for default data (shaded box), $P_{i-l} = 0$ (+), and $P_{2i-l} = 0$ (*): A. The association curves used to determine the association rate constants (listed in Table 3) for the IL-2-α receptor complex for default data (shaded box), $P_{i-l} = 0$ (+), and $P_{2i-l} = 0$ (*): B. The association curves used to determine the association rate constants (listed in Table) for the IL-2-α receptor complex for default data (shaded box), $P_{i-l} = 0$ (+), and $P_{2i-l} = 0$ (*): C. The association rate constants for the

binding of IL-2 by the α receptor are determined from the initial slope as shown by Landgraf, et al.[14].

FIGURE 3. Ligand - receptor association curves. The association of IL-2 and α receptors for $P_{i-l} = 0$ and $r = 1x10^{-6}m$ (shaded box), $P_{2i-l} = 0$ and $r = 1x10^{-6}m$ (+), $P_{i-l} = 0$ and $r = 1x10^{-5}m$ (*), and $P_{2i-l} = 0$ and $r = 1x10^{-5}m$ (empty box): A. The association curves used to determine the association rate constants (listed in Table) for $P_{i-l} = 0$ and $r = 1x10^{-6}m$ (shaded box) and $P_{i-l} = 0$ and $r = 1x10^{-5}m$ (+): B. The association curves used to determine the association rate constants (listed in Table 3) for $P_{2i-l} = 0$ and $r = 1x10^{-6}m$ (shaded box) and $P_{2i-l} = 0$ and $r = 1x10^{-5}m$ (+): C. The association rate constants for the binding of IL-2 by the α receptor are determined from the initial slope as shown by Landgraf, et al. [14].

FIGURE 4. Ligand - receptor association curves. The relationship between the number of IL-2-α receptor complexes and the number of non-specifically bound ligand is shown for a cell radius of $1x10^{-6}m$ (shaded box for IL-2-α and + for g-l): A. The relationship between the number of IL-2-α receptor complexes and the number of non-specifically bound ligand is shown for a cell radius of $1x10^{-5}m$ (shaded box for IL-2-α and + for g-l): B.

FIGURE 5. Ligand - receptor association and dissociation curves. The association

curves for the binding of IL-2 by the α receptor for $P_{g-l} = 0$, $P_{i-l} = 0$, $P_{j-l} = 0$, and $r = 1x10^{-6}m$ (shaded box) and $P_{g-l} = 0$, $P_{2i-l} = 0$, $P_{2j-l} = 0$, and $r = 1x10^{-6}m$ (+): A. The association curves for the binding of IL-2 by the α receptor for $P_{g-l} = 0$, $P_{i-l} = 0$, $P_{j-l} = 0$, and $r = 1x10^{-5}m$ (shaded box) and $P_{g-l} = 0$,$P_{2i-l} = 0$, $P_{2j-l} = 0$, and $r = 1x10^{-5}m$ (+): B.

FIGURE 6. Kinetics of ligand dissociation. The dissociation of IL-2 at non-specific sites: shaded box, at the α receptor on cells of radius $1x10^{-6}m$: empty box, at the α receptor on cells of radius $1x10^{-5}m$: vertical line. The dissociation rate constants determined from the slopes of the curves are listed in Table 3 and the half-lives determined from the dissociation rate constants are listed in Table 3.

FIGURE 7. Ligand - receptor association curves. The association curves for the binding of IL-2 by the α receptor for $r = 1x10^{-6}m$and$D_{ligand} = 1x10^{-10}m^2s^{-1}$(shaded box), $r = 1x10^{-6}m$ and $D_{ligand} = 1x10^{-15}m^2s^{-1}$(+), and $r = 1x10^{-6}m$ and $D_{ligand} = 1x10^{-5}m^2s^{-1}$(*): A. The association curves for the binding of IL-2 by the α receptor for $r = 1x10^{-5}m$ and $D_{ligand} = 1x10^{-10}m^2s^{-1}$(shaded box), $r = 1x10^{-5}m$ and $D_{ligand} = 1x10^{-15}m^2s^{-1}$(+), and $r = 1x10^{-5}m$ and $D_{ligand} = 1x10^{-5}m^2s^{-1}$(*): B.

FIGURE 8. Ligand - receptor association curves. The association curves for the binding of IL-2 by the α receptor for $[ligand]_o = 0$ and number $g-l_o = 100000$(shaded

box) and for $[ligand]_o = 0$, number $g - l_o = 100000$, and $P_{i-l} = 0$ (+).

FIGURE 9. Ligand - receptor association curves for the autocrine growth system and identical receptors. The legend for all curves is shaded box: i-l, +: i-j, *:(i-j)-l, empty box: (i-j)...l. Default Data: A. Elimination of ligand-receptor associations: B. Elimination of preformed heterodimer: C.

FIGURE 10. Ligand - receptor association curves for the autocrine/paracrine growth system and identical receptors. The legend for all curves is shaded box: i-l, +: i-j, *:(i-j)-l, empty box: (i-j)...l. Default Data: A. Elimination of ligand-receptor associations: B. Elimination of preformed heterodimer: C.

FIGURE 11. Ligand - receptor association curves for the paracrine growth system and identical receptors. The legend for all curves is shaded box: i-l, +: i-j, *:(i-j)-l, empty box: (i-j)...l. Default Data: A. Elimination of ligand-receptor associations: B. Elimination of preformed heterodimer: C.

FIGURE 12. First order kinetic plots for the dissociation of g-l (shaded box), i-j (+), i-l (empty box), and (i-j)-l (*). The dissociation constants are listed in Table 3.

FIGURE 13. Ligand - receptor association curves for the autocrine growth system

and non-identical receptors. The legend for all curves is shaded box: i-l, +: j-l, *:i-j, empty box: (i-j)-l, x:(i- j)...l. Default Data: A. Elimination of ligand-receptor associations: B. Elimination of preformed heterodimer: C.

FIGURE 14. Ligand - receptor association curves for the autocrine/paracrine growth system and non-identical receptors. The legend for all curves is shaded box: i-l, +: j-l, *:i-j, empty box: (i-j)-l, x:(i-j)...l. Default Data: A. Elimination of ligand- receptor associations: B. Elimination of preformed heterodimer: C.

FIGURE 15. Ligand - receptor association curves for the paracrine growth system and non-identical receptors. The legend for all curves is shaded box: i-l, +: j-l, *:i-j, empty box: (i-j)-l, x:(i- j)...l. Default Data: A. Elimination of ligand-receptor associations: B. Elimination of preformed heterodimer: C.

References

[1] Waite, B.A. 1993. A Diffusion-Kinetics Model for Receptor/Ligand Interactions at Cell Surfaces. Manuscript.

[2] Waite, B.A., and J D. Stewart. 1992. An idealized dynamical model of simple diffusional interactions between macromolecules and between macromolecules and surfaces. Mathematical Biosciences, in press.

[3] Darnell, James; Lodish, Harv ·; Baltimore, David, *Molecular Cell Biology* ; Scientific American Books: New York, 1986; p. 667- 669.

[4] Singer, S.J. and Micolson, G.L., "The Fluid Mosaic Model of the Structure of Cell Membranes," Science 173, p. 720-731 (1972).

[5] Golub, Edward S. and Green, Douglas R, *Immunology: A Synthesis*, 2nd Edition; Sinauer Associates, Inc: Sunderland, Massachussetts, 1991, p. 456.

[6] Smith, K.A., Science 240, p.1169-1176 (1988).

[7] Caligiuri, M., Zmuidzinas, A., Manley, T.J., Levine, H., Smith, K.A., and Ritz, J., J. Exp. Med. 171, p. 1509-1526 (1990).

[8] Golub, Edward S. and Green, Douglas R, *Immunology: A Synthesis*, 2nd Edition; Sinauer Associates, Inc: Sunderland, Massachussetts, 1991, p. 453.

[9] Smith, K.A., Ann. Rev. Cell Biol. 5, p. 397-425 (1989).

[10] Golub, Edward S. and Green, Douglas R, *Immunology: A Synthesis*, 2nd Edition; Sinauer Associates, Inc: Sunderland, Massachussetts, 1991, p. 455.

[11] Golub, Edward S. and Green, Douglas R, *Immunology: A Synthesis*, 2nd Edition; Sinauer Associates, Inc: Sunderland, Massachussetts, 1991, p. 454.

[12] Wang, H.M., and Smith, K.A., J. Exp. Med. 166, p. 239-243 (1989).

[13] Teshigawara, K., Wang, H.M., Kato, K., and Smith, K.A., J. Exp. Med. 165 p. 223-238 (1987).

[14] Landgraf, B.E., D.P. Williams, J.R. Murphy, T.R. Sana, K.A. Smith, and T.L. Ciardelli. 1992. Working Manuscript.

[15] Goldstein, B., D. Jones, I.G. Kevrekidis, and A.S. Perelson.1992. Evidence for p55-p75 heterodimers in the absence of interleukin-2 from Scatchard Plot Analysis. International Immunology, 4:23-32.

[16] Kamio, M., T. Uchiyama, N. Arima, K. Itoh, T. Ishikawa, T. Hori, and H. Uchino. 1990. Role of chain-IL-2 complex in the formation of the ternary complex of IL-2 and high-affinity IL-2 receptor. International Immunology, 2:521-530.

[17] Saragovi, H. and T.R. Malek. 1988. Direct identification of the murine IL-2 receptor p55-p75 heterodimer in the absence of IL-2. Journal of Immunology, 141:476-482

[18] Grant, A.J., E. Roessler, G. Ju, M. Tsudo, K. Sugamura, T.A. Waldmann. 1992. The interleukin-2 receptor (IL-2R): The IL-2R subunit alters the function of the IL-2R subunit to enhance IL-2 binding and signaling by mechanisms that do not require binding of IL-2 to IL-2R subunit. Proc. Natl. Acad. Sci., USA, 89:2165-2169

Table 1

Table 1A
Species of the Simple Model

species number	species symbol	description
1	l	bulk free interleukin-2 ligand
2	i	Il-2 alpha receptor
3	j	Il-2 beta receptor
4	i-l	ligand bound to Il-2 alpha receptor
5	j-l	ligand bound to Il-2 beta receptor
6	g-l	ligand non-specifically bound to cell surface
7	i_l	ligand rebounding from the Il-2 alpha receptor
8	j_l	ligand rebounding from the Il-2 beta receptor
9	g_l	ligand rebounding from a non-specific binding site
10	i_g-l	non-specifcally bound ligand rebounding from Il-2 alpha receptor on the cell membrane
11	j_g-l	non-specifcally bound ligand rebounding from Il-2 beta receptor on the cell membrane

Table 1B
Species of the Complex Model

The complex model includes all of the species of the simple model and the following additional species

species number	species symbol	description
12	i-j	heterodimer of Il-2 alpha and Il-2 beta receptors
13	i_j	rebounding encounter between Il-2 alpha and Il-2 beta receptors
14	i_j-l	Il-2 alpha receptor rebounding from the Il-2 beta receptor-ligand complex
15	j_i-l	Il-2 beta receptor rebounding from the Il-2 alpha receptor-ligand complex
16	(i-j)-l	interleukin-2/Il-2 alpha receptor/Il-2 beta receptor signalling complex
17	(i-j)_l	ligand rebounding from the Il-2 alpha receptor/Il-2 beta receptor heterodimer

Table 2: Experimental Parameters

	Value			
		Complex Model		
Parameter	Simple Model	Identical Receptors	Non-Ident Receptors	Description
Pil	0.8	0.3	0.3	Probability of binding for i+1 via ligand-surface mechanism
Pjl	0.8	0.3	0.1	Probability of binding for j+1 via ligand-surface mechanism
Pgl	0.5	0.5	0.5	Probability of binding for g+1 via ligand-surface mechanism
P2il	0.5	0.5	0.5	Probability of binding for i+1 via membrane-bound diffusion mechanism
P2jl	0.5	0.5	0.2	Probability of binding for j+1 via membrane-bound diffusion mechanism
Pij	n/a	0.5	0.5	Probability of binding for i+j via membrane-bound diffusion mechanism
Pijl	n/a	0.5	0.5	Probability of binding to form (i-j)-1 via a ligand surface or membrane-bound diffusion mechanism

Table 3: Summary of Kinetic Data

Association Rate Constants
1/(second*M)

radius	Simple Model 1 micron i-l	10 micron i-l	1 micron j-l	Previously Reported[14] i-l	Complex Model 1 micron (i-j)-l	Prev. Reported [14] (i-j)-l
default	4.52E+06	4.52E+07	4.52E+06	1.20E+07	8.79E+10	1.20E+08
pil=0	4.42E+06	4.21E+07	4.54E+06	n/a	n/a	n/a
p2il=0	2.47E+05	2.87E+04	8.96E+06	n/a	n/a	n/a

Dissociation Rate Constants
1/seconds

	i-l	g-l	i-j	(i-j)-l
Simple Model	2.02E-03	1.00E-03	n/a	n/a
Complex Model	2.02E-03	9.90E-04	8.10E-04	4.04E-03
Landgraf	4.50E-02	n/a	n/a	1.60E-04

Half-Lives
seconds

	i-l	g-l	i-j	(i-j)-l
Simple Model	3.43E+02	6.92E+02	n/a	n/a
Complex Model	3.43E+02	6.98E+02	8.56E+02	1.71E+02
Landgraf	1.54E+01	n/a	n/a	4.33E+03

Figure 1A

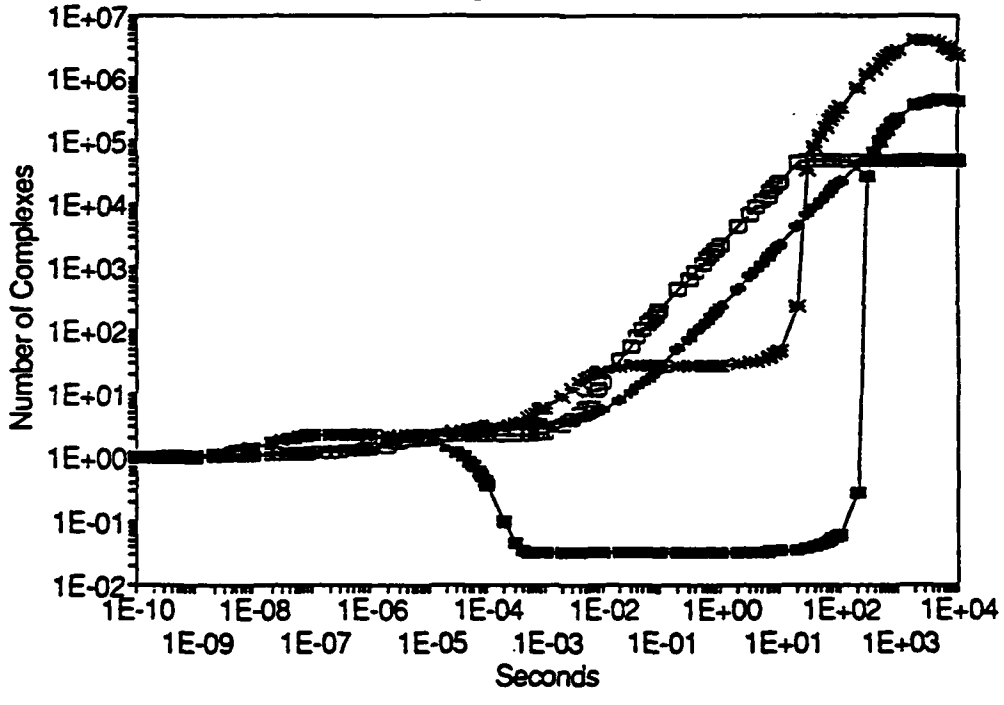
1E+07
1E+06
1E+05
1E+04
1E+03
1E+02
1E+01
1E+00
1E-01
1E-02
Number of Complexes
1E-10
1E-09
1E-08
1E-07
1E-06
1E-05
1E-04
1E-03
1E-02
1E-01
1E+00
1E+01
1E+02
1E+03
1E+04
Seconds

Figure 1B

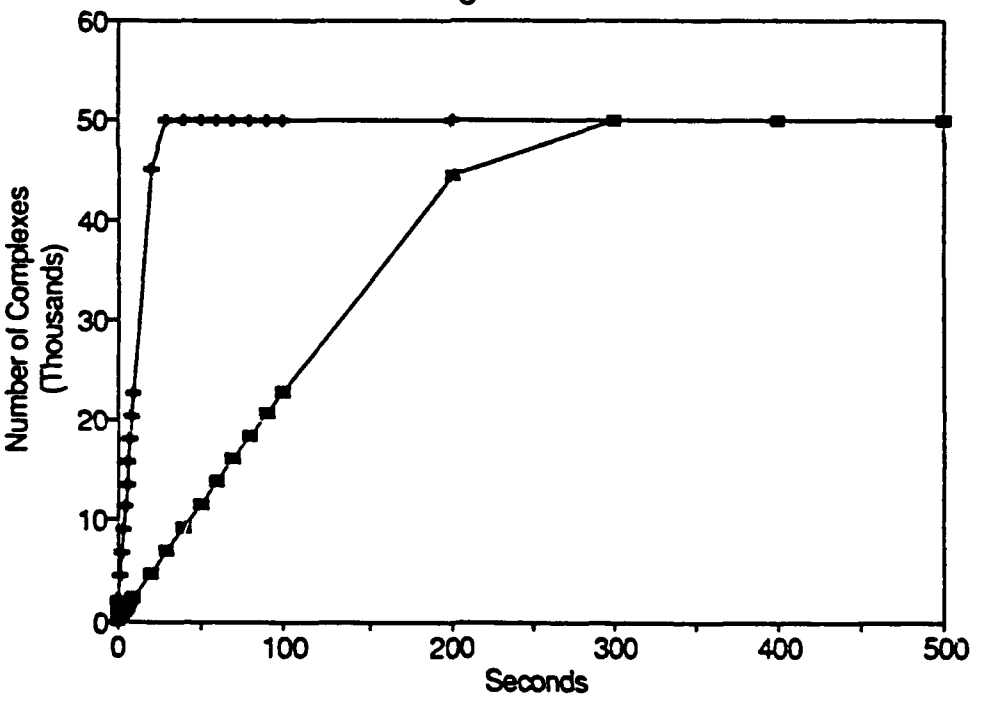
60
50
40
30
20
10
0
Number of Complexes (Thousands)
0
100
200
300
400
500
Seconds

Figure 1C

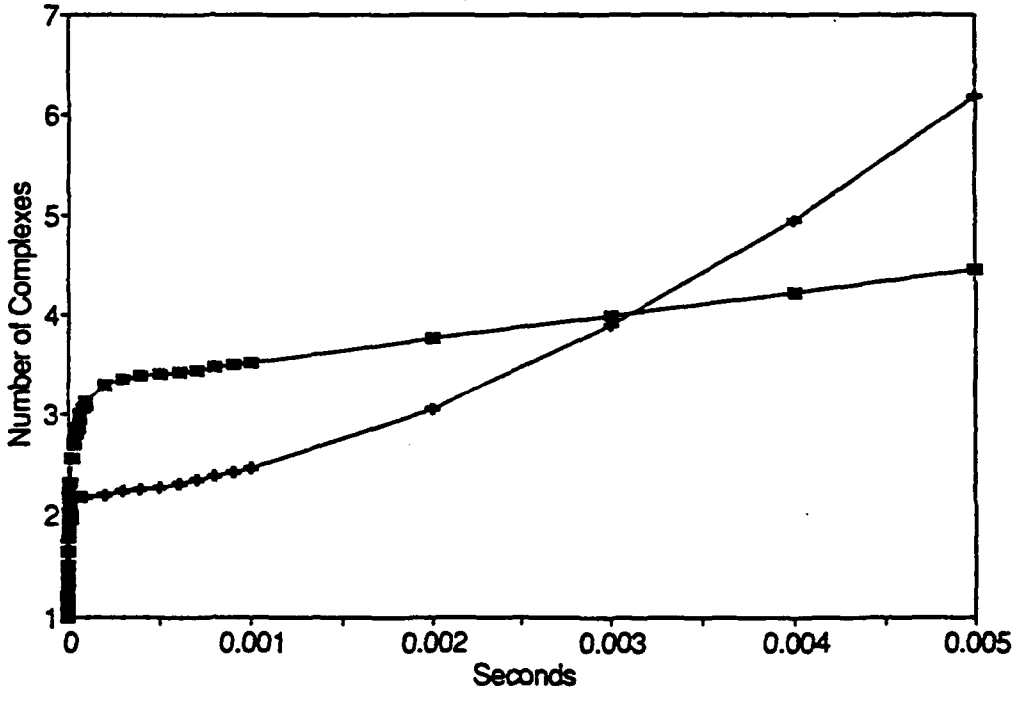
Number of Complexes
7
6
5
4
3
2
1
0
0.001
0.002
0.003
0.004
0.005
Seconds

Figure 2A

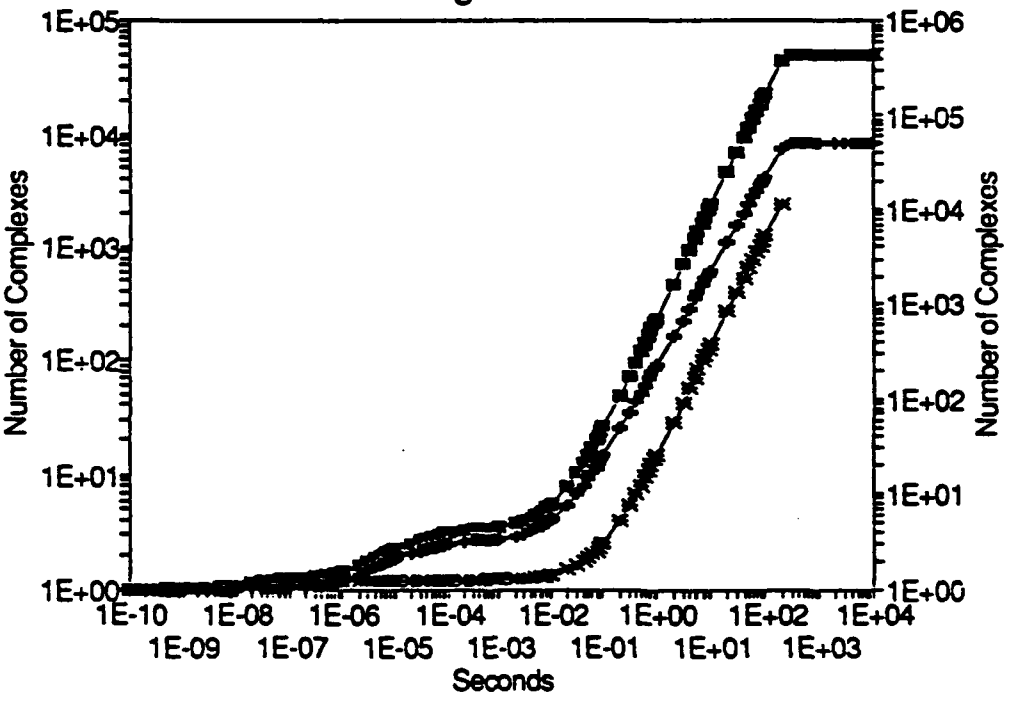
1E+05
1E+04
1E+03
1E+02
1E+01
1E+00
Number of Complexes
1E+06
1E+05
1E+04
1E+03
1E+02
1E+01
1E+00
Number of Complexes
1E-10 1E-08 1E-06 1E-04 1E-02 1E+00 1E+02 1E+04
1E-09 1E-07 1E-05 1E-03 1E-01 1E+01 1E+03
Seconds

Figure 2B

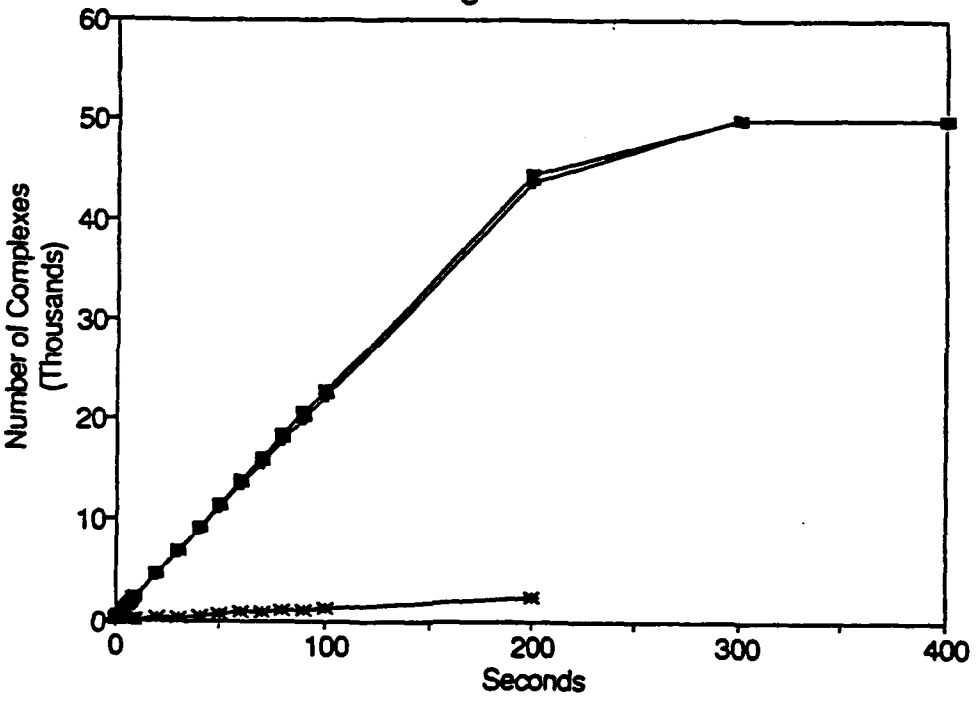
Number of Complexes
(Thousands)
60
50
40
30
20
10
0
0
100
200
300
400
Seconds

Figure 2C

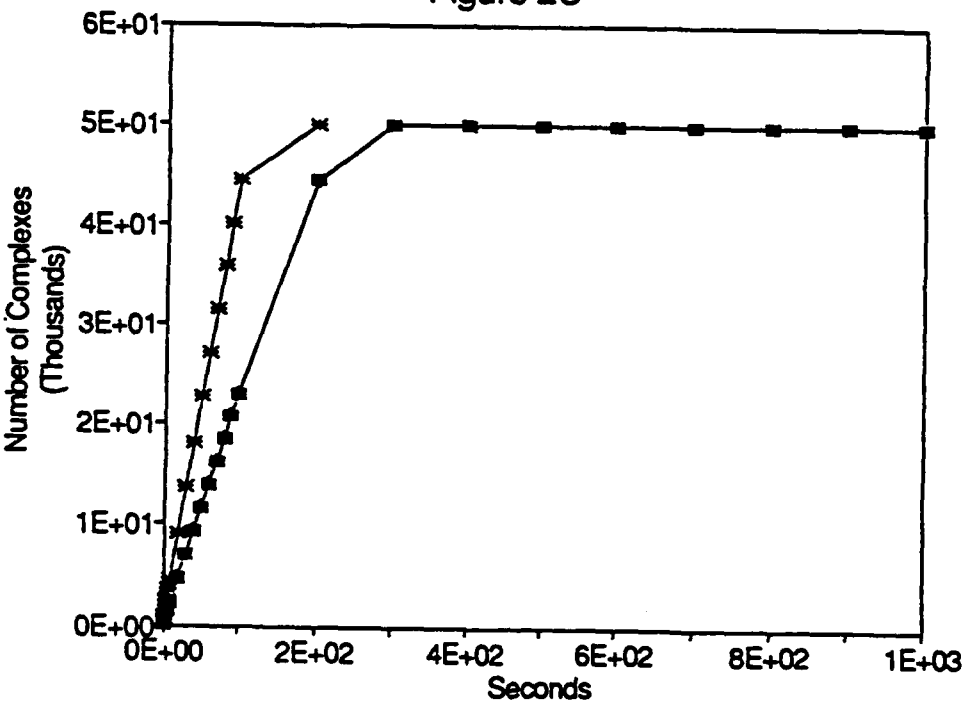
6E+01
5E+01
4E+01
3E+01
2E+01
1E+01
0E+00
Number of Complexes (Thousands)
0E+00
2E+02
4E+02
6E+02
8E+02
1E+03
Seconds

Figure 3A

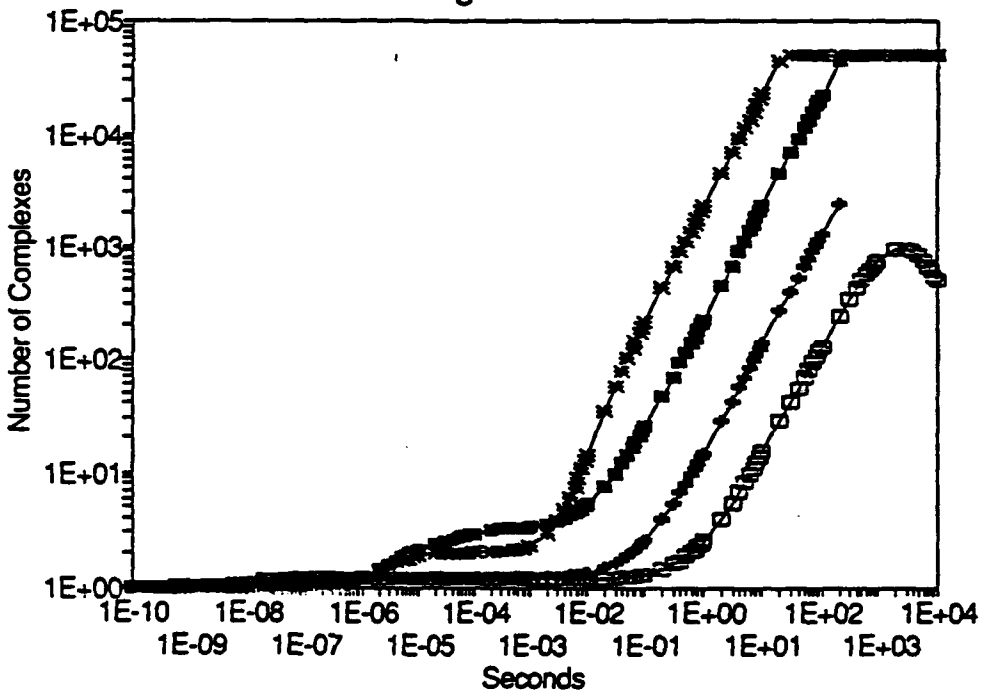
1E+05
1E+04
1E+03
1E+02
1E+01
1E+00
Number of Complexes
1E-10
1E-09
1E-08
1E-07
1E-06
1E-05
1E-04
1E-03
1E-02
1E-01
1E+00
1E+01
1E+02
1E+03
1E+04
Seconds

Figure 3B

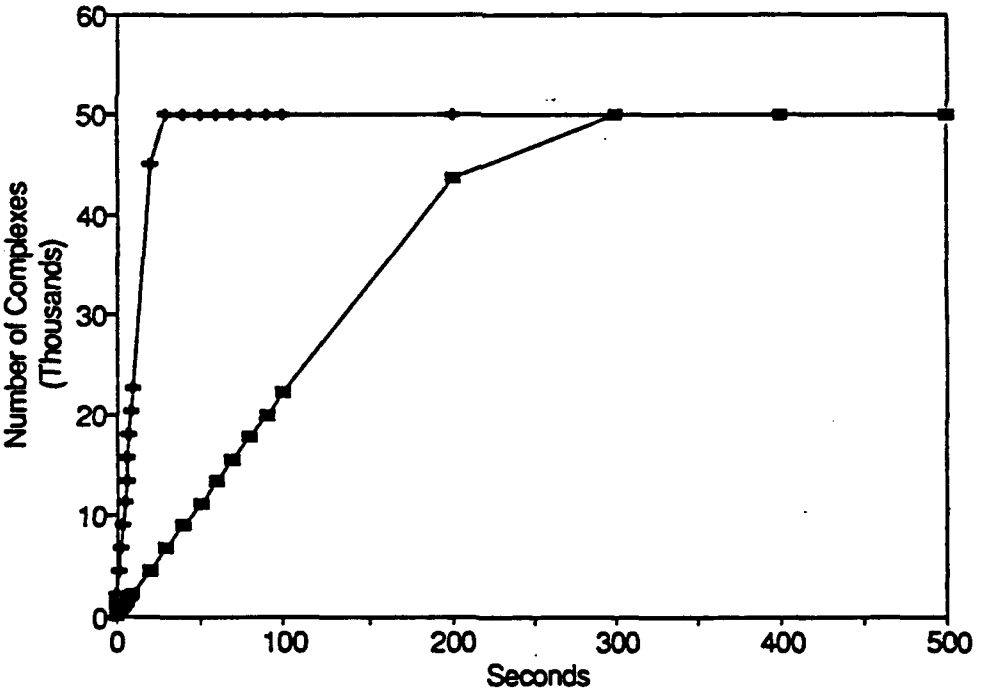
60
50
40
30
20
10
0
Number of Complexes (Thousands)
0
100
200
300
400
500
Seconds

Figure 3C

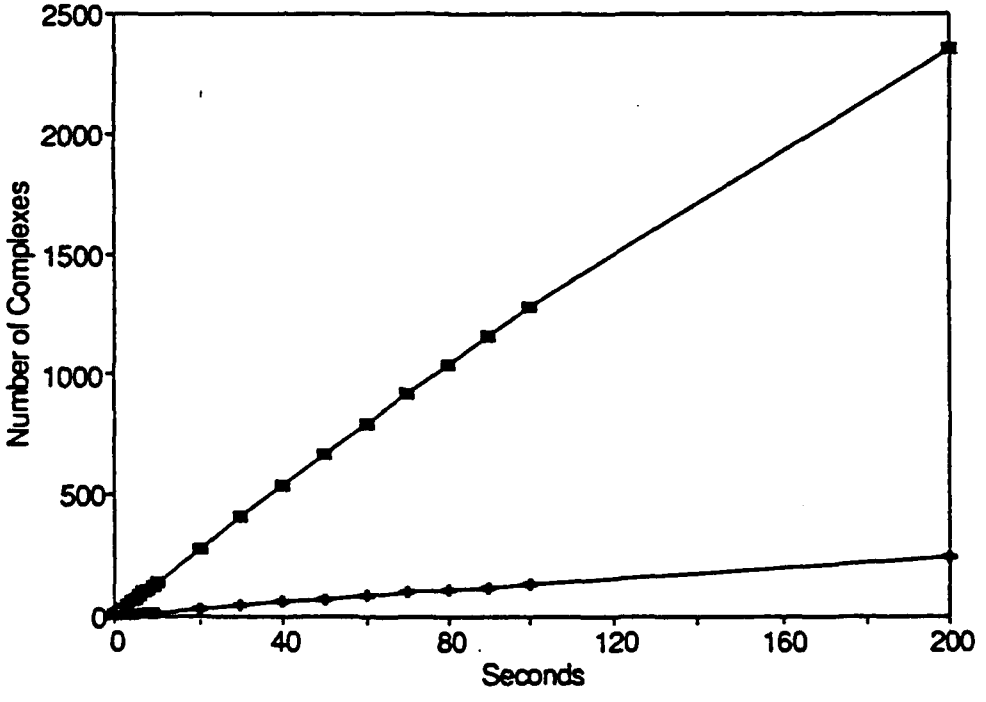
2500
2000
1500
1000
500
0
Number of Complexes
0
40
80
120
160
200
Seconds

Figure 4A

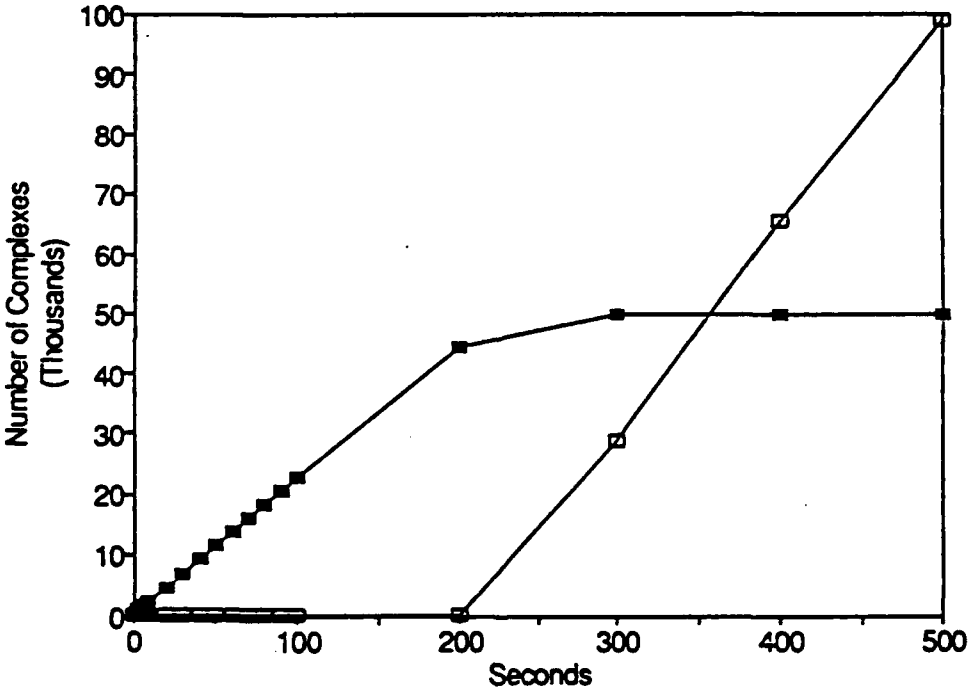
Number of Complexes (Thousands)
100
90
80
70
60
50
40
30
20
10
0
0
100
200
300
400
500
Seconds

Figure 4B

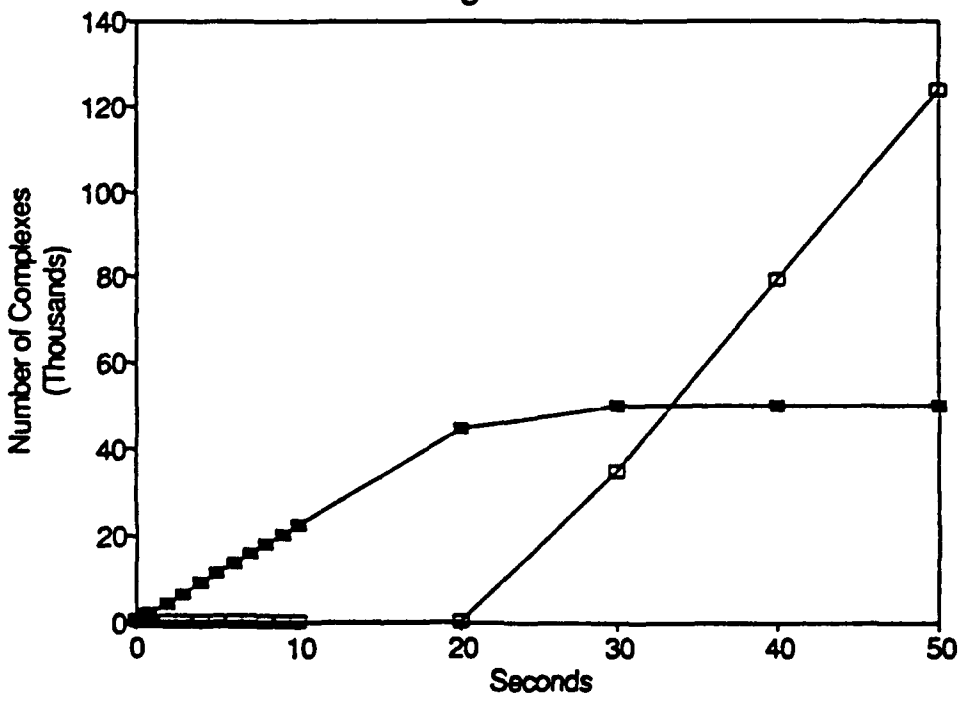
140
120
100
80
60
40
20
0
Number of Complexes (Thousands)
0
10
20
30
40
50
Seconds

Figure 5A

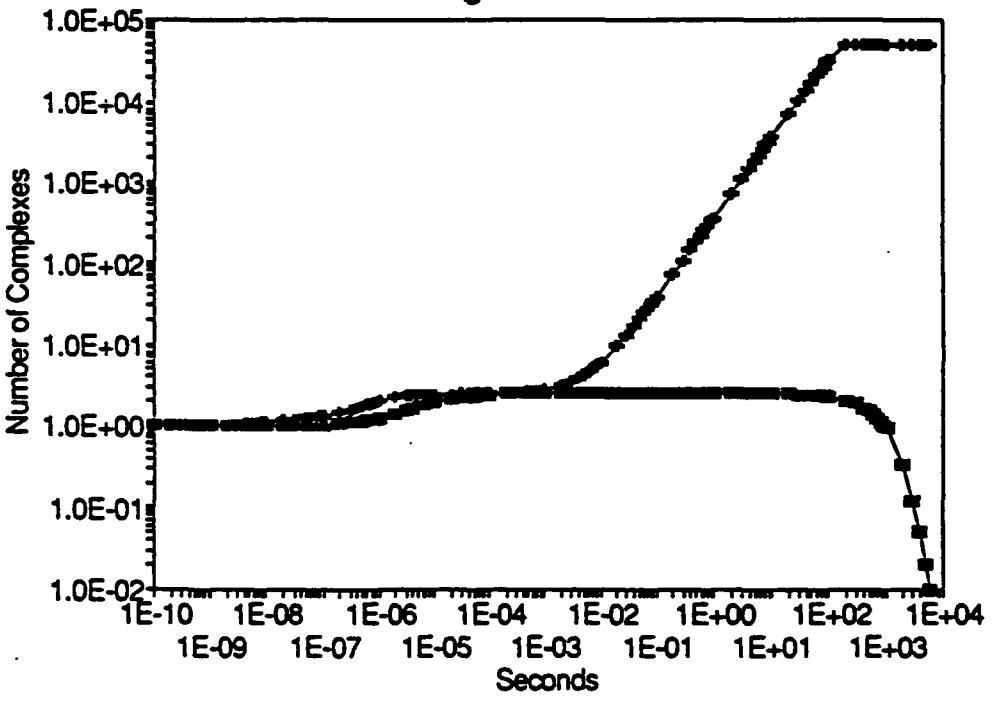
1.0E+05
1.0E+04
1.0E+03
1.0E+02
1.0E+01
1.0E+00
1.0E-01
1.0E-02
Number of Complexes
1E-10
1E-09
1E-08
1E-07
1E-06
1E-05
1E-04
1E-03
1E-02
1E-01
1E+00
1E+01
1E+02
1E+03
1E+04
Seconds

Figure 5B

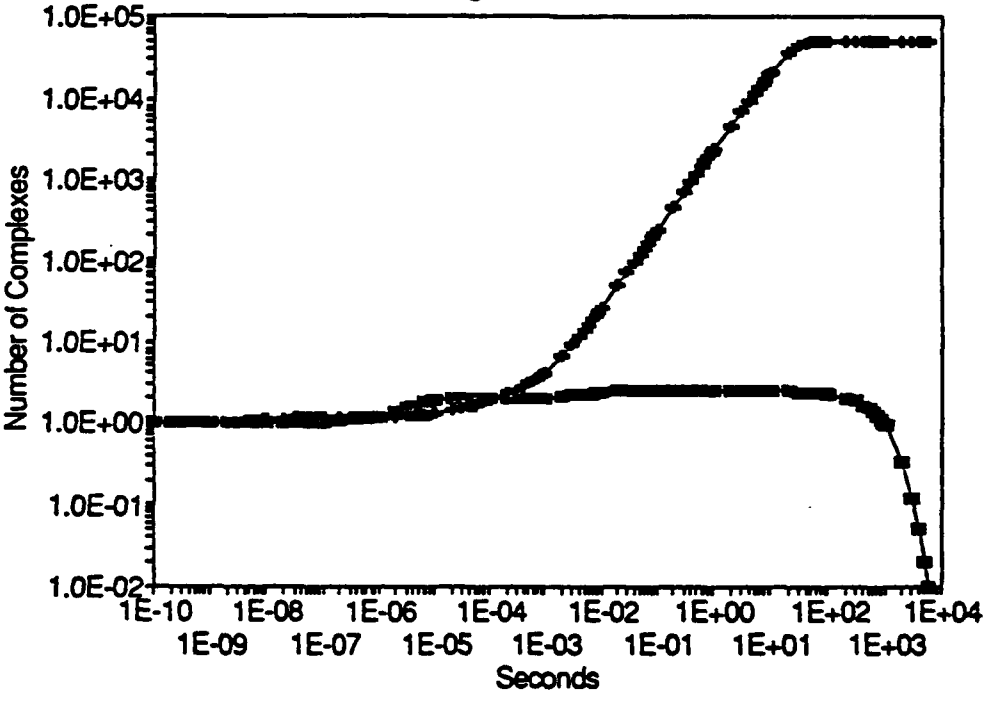
1.0E+05
1.0E+04
1.0E+03
1.0E+02
1.0E+01
1.0E+00
1.0E-01
1.0E-02
Number of Complexes
1E-10
1E-09
1E-08
1E-07
1E-06
1E-05
1E-04
1E-03
1E-02
1E-01
1E+00
1E+01
1E+02
1E+03
1E+04
Seconds

Figure 6

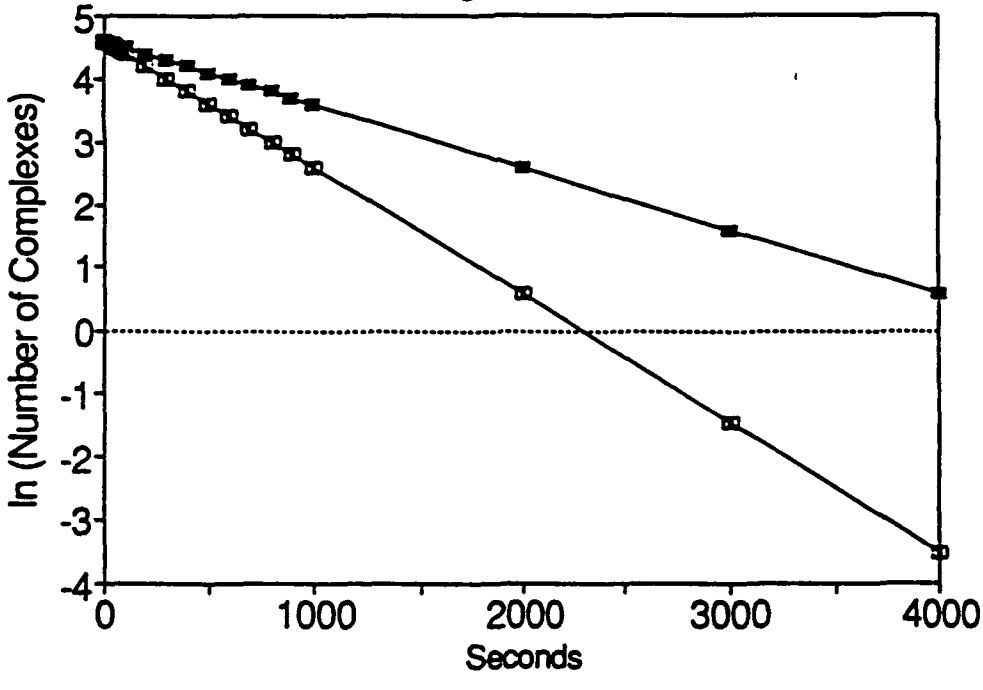
5
4
3
2
1
0
-1
-2
-3
-4
ln (Number of Complexes)
0
1000
2000
3000
4000
Seconds

Figure 7A

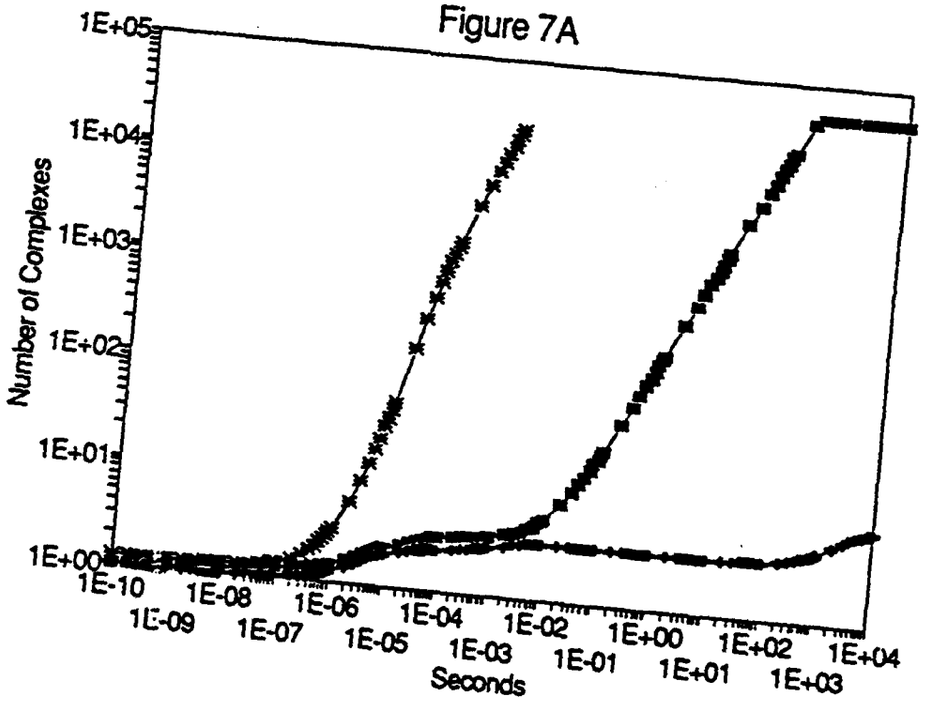
1E+05
1E+04
1E+03
1E+02
1E+01
1E+00
Number of Complexes
1E-10
1E-09
1E-08
1E-07
1E-06
1E-05
1E-04
1E-03
1E-02
1E-01
1E+00
1E+01
1E+02
1E+03
1E+04
Seconds

Figure 7B

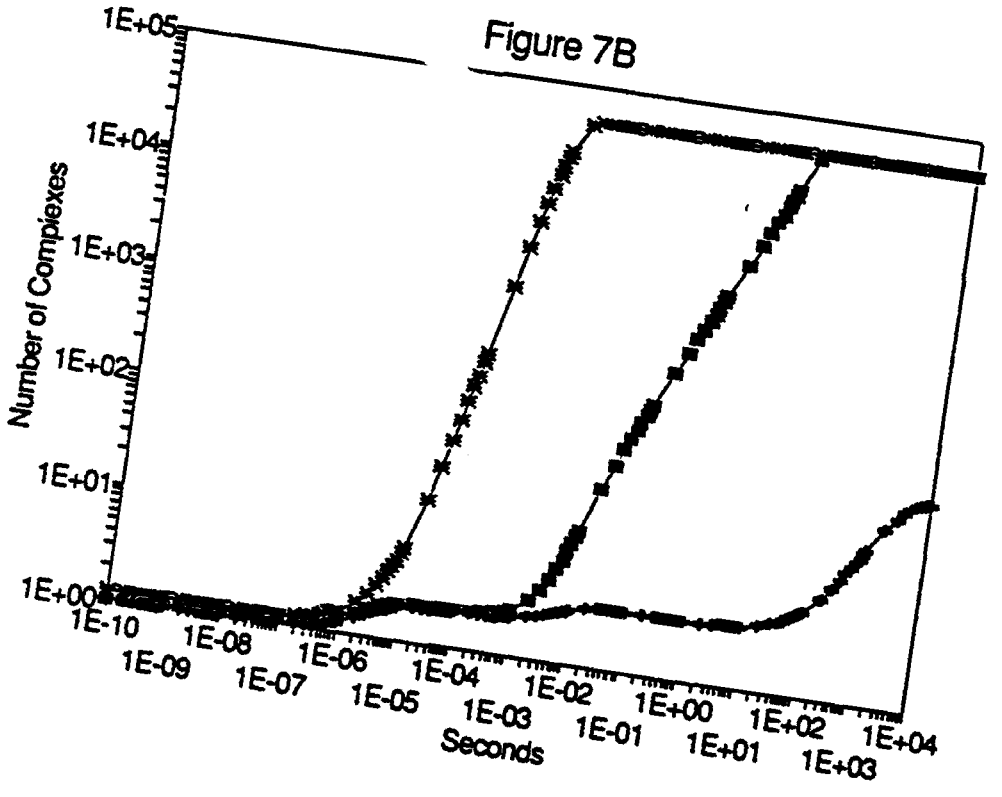
Number of Complexes
1E+05
1E+04
1E+03
1E+02
1E+01
1E+00
1E-10
1E-09
1E-08
1E-07
1E-06
1E-05
1E-04
1E-03
1E-02
1E-01
1E+00
1E+01
1E+02
1E+03
1E+04
Seconds

Figure 8

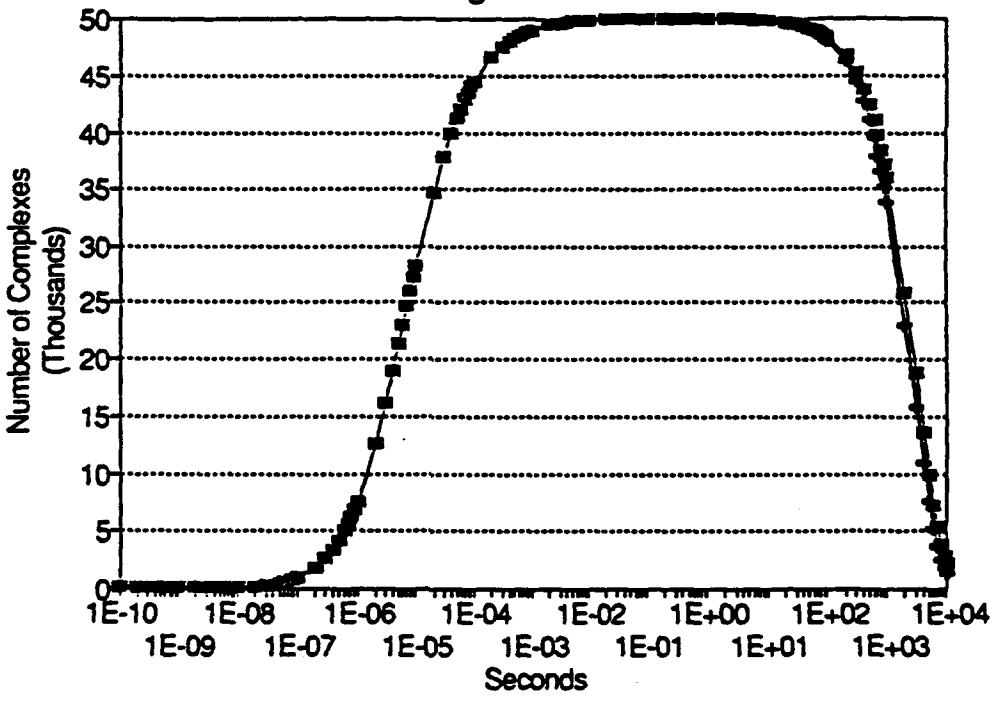
Number of Complexes (Thousands)
50
45
40
35
30
25
20
15
10
5
0
1E-10
1E-09
1E-08
1E-07
1E-06
1E-05
1E-04
1E-03
1E-02
1E-01
1E+00
1E+01
1E+02
1E+03
1E+04
Seconds

Figure 9A

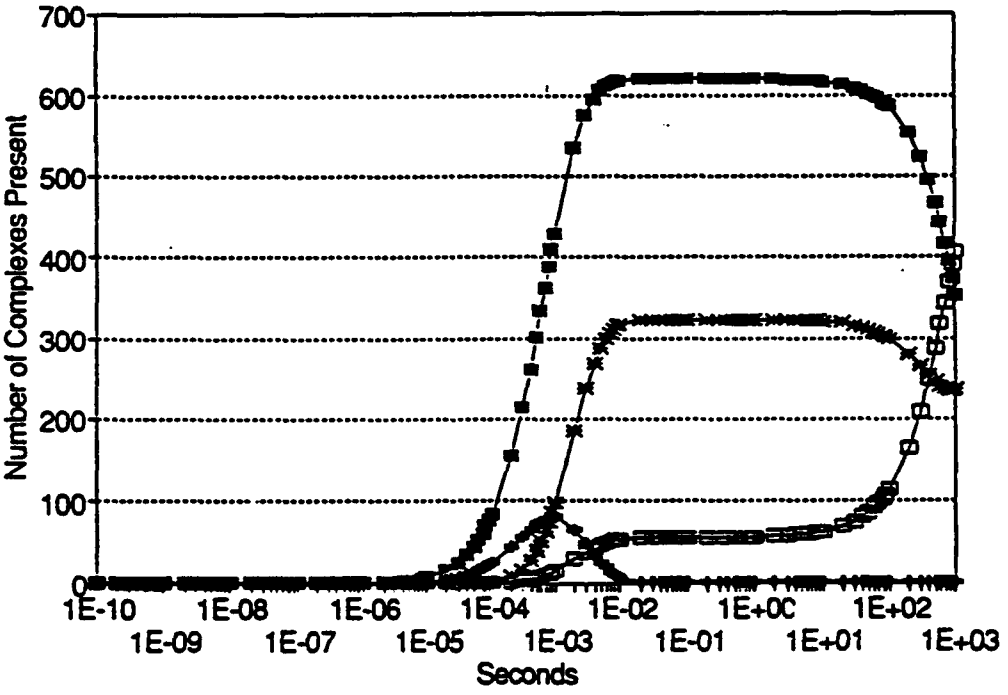
700
600
500
400
300
200
100
0
Number of Complexes Present
1E-10
1E-09
1E-08
1E-07
1E-06
1E-05
1E-04
1E-03
1E-02
1E-01
1E+00
1E+01
1E+02
1E+03
Seconds

Figure 9B

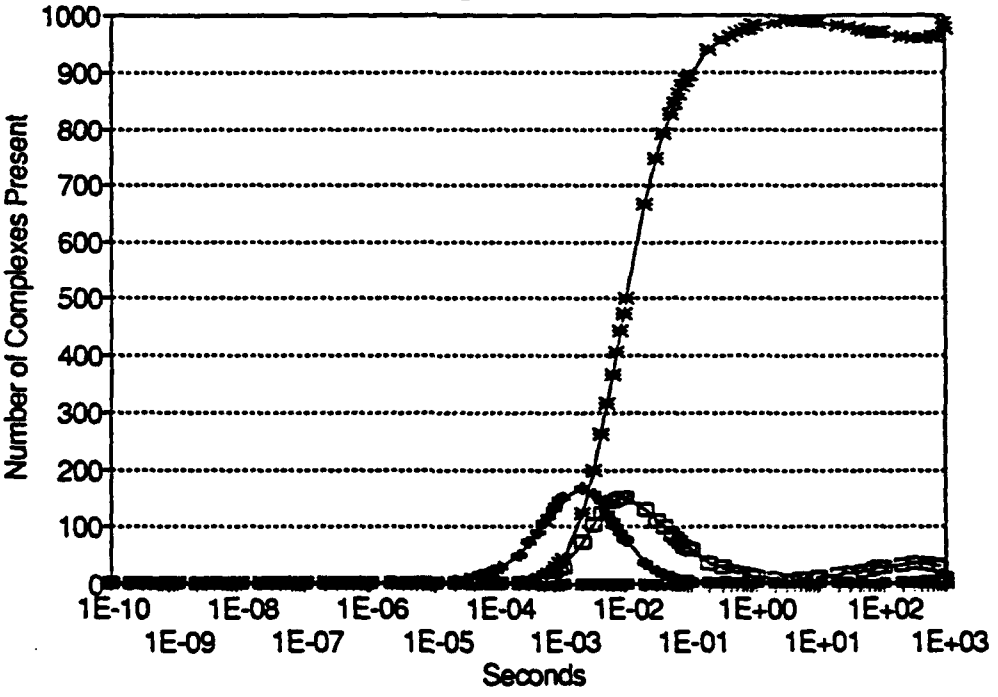
Number of Complexes Present
1000
900
800
700
600
500
400
300
200
100
0
1E-10
1E-09
1E-08
1E-07
1E-06
1E-05
1E-04
1E-03
1E-02
1E-01
1E+00
1E+01
1E+02
1E+03
Seconds

Figure 9C

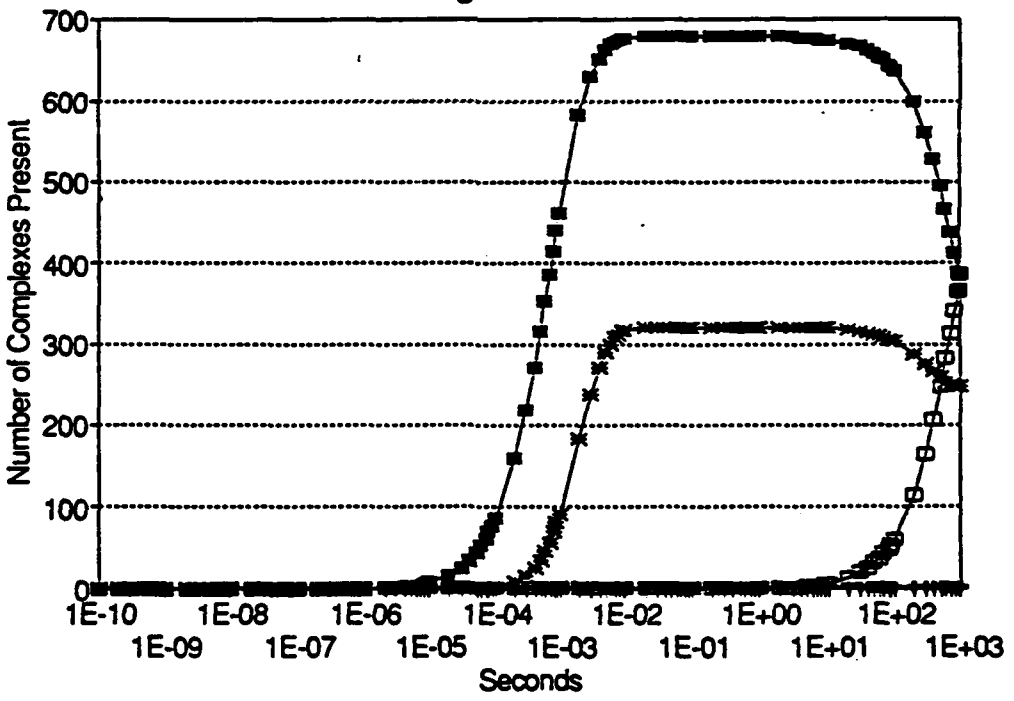
700
600
500
400
300
200
100
0
Number of Complexes Present
1E-10
1E-09
1E-08
1E-07
1E-06
1E-05
1E-04
1E-03
1E-02
1E-01
1E+00
1E+01
1E+02
1E+03
Seconds

Figure 10A

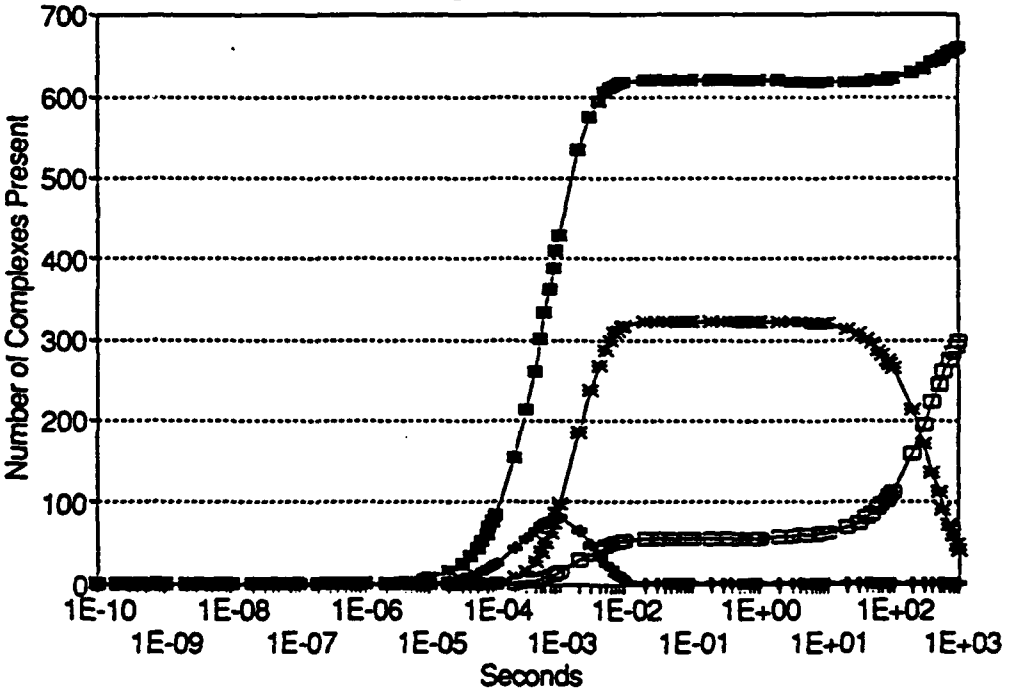
700
600
500
400
300
200
100
0
Number of Complexes Present
1E-10
1E-09
1E-08
1E-07
1E-06
1E-05
1E-04
1E-03
1E-02
1E-01
1E+00
1E+01
1E+02
1E+03
Seconds

Figure 10B

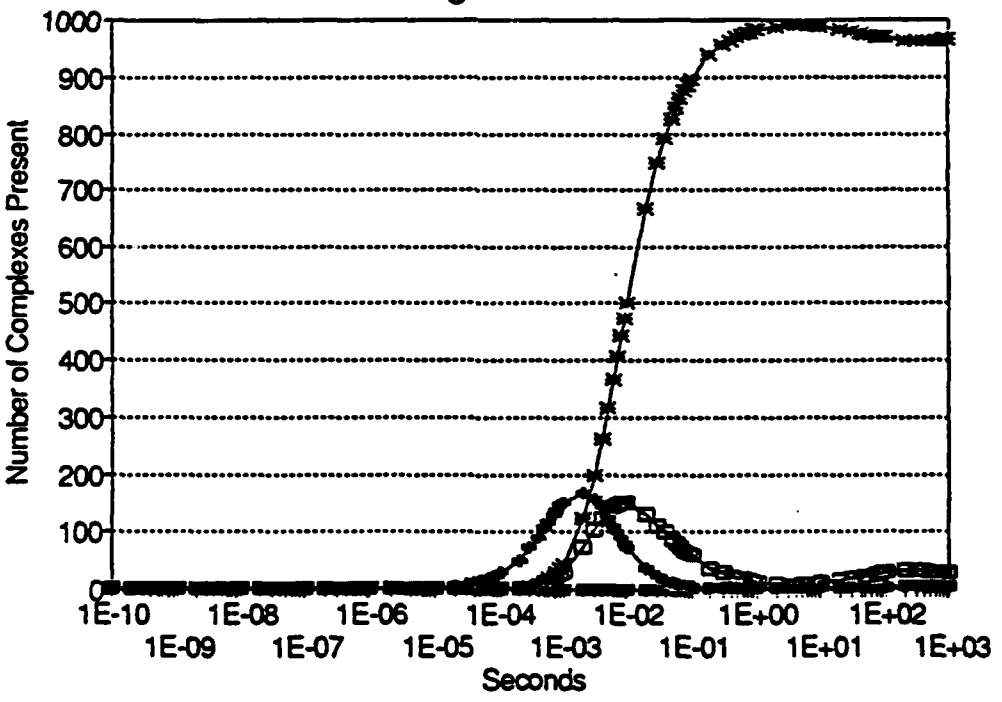
Number of Complexes Present
1000
900
800
700
600
500
400
300
200
100
0
1E-10
1E-09
1E-08
1E-07
1E-06
1E-05
1E-04
1E-03
1E-02
1E-01
1E+00
1E+01
1E+02
1E+03
Seconds

Figure 10C

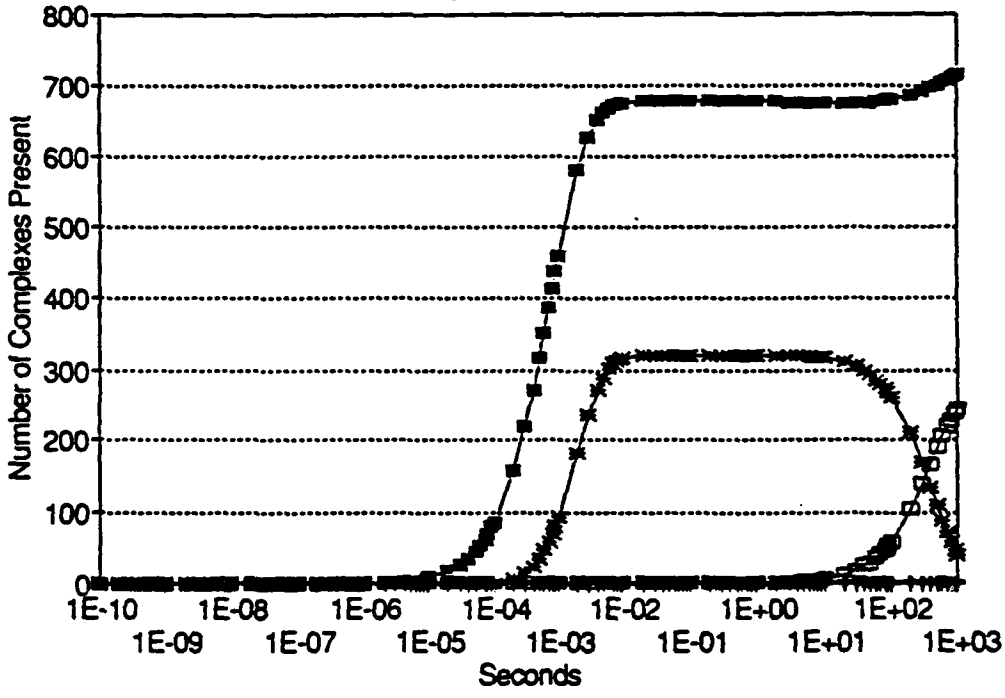
800
700
600
500
400
300
200
100
0
Number of Complexes Present
1E-10
1E-09
1E-08
1E-07
1E-06
1E-05
1E-04
1E-03
1E-02
1E-01
1E+00
1E+01
1E+02
1E+03
Seconds

Figure 11A

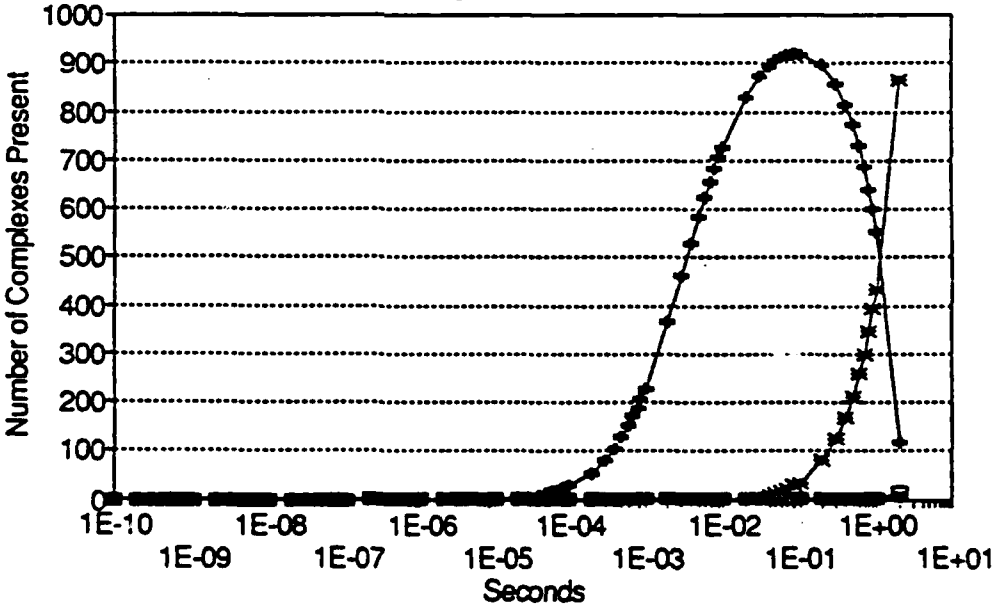
Number of Complexes Present
1000
900
800
700
600
500
400
300
200
100
0
1E-10
1E-09
1E-08
1E-07
1E-06
1E-05
1E-04
1E-03
1E-02
1E-01
1E+00
1E+01
Seconds

Figure 11B

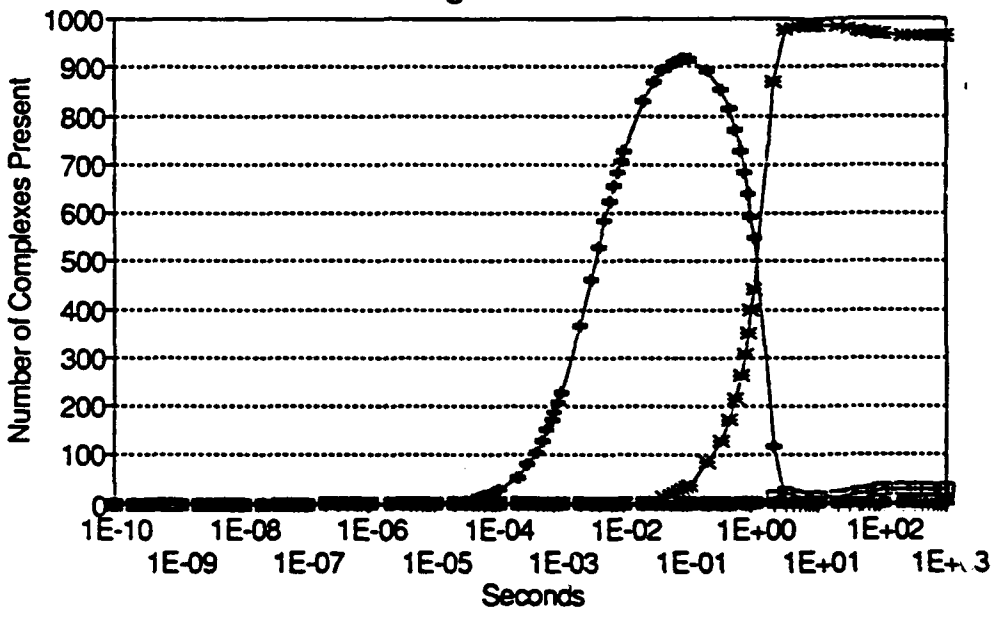
1000
900
800
700
600
500
400
300
200
100
0
Number of Complexes Present
1E-10
1E-09
1E-08
1E-07
1E-06
1E-05
1E-04
1E-03
1E-02
1E-01
1E+00
1E+01
1E+02
Seconds

Figure 12

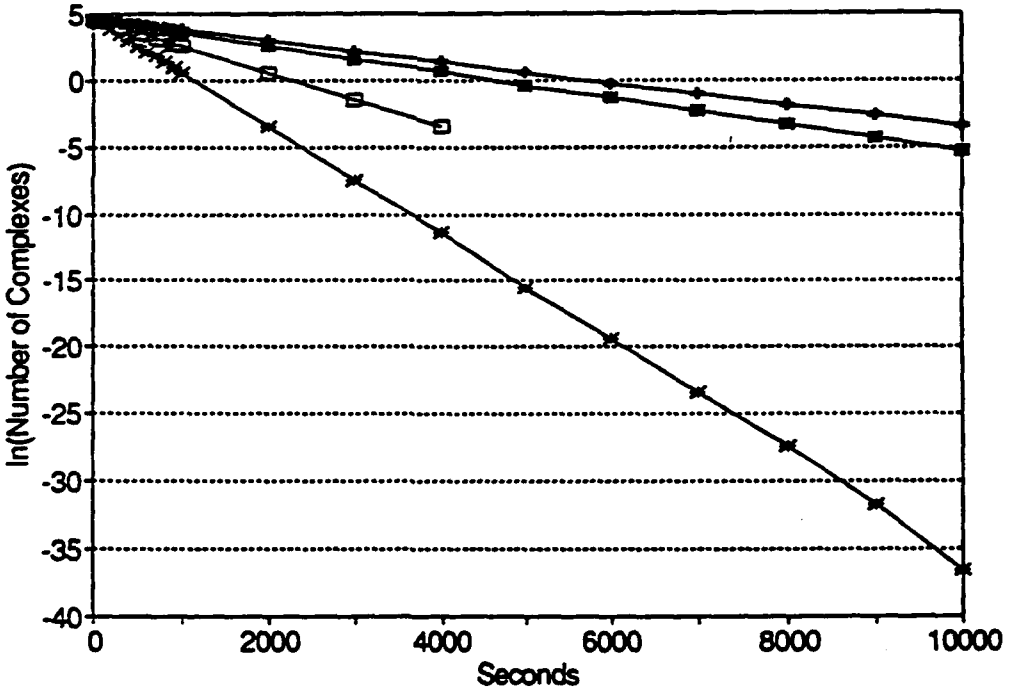
5
0
-5
-10
-15
-20
-25
-30
-35
-40
ln(Number of Complexes)
0
2000
4000
6000
8000
10000
Seconds

Figure 13A

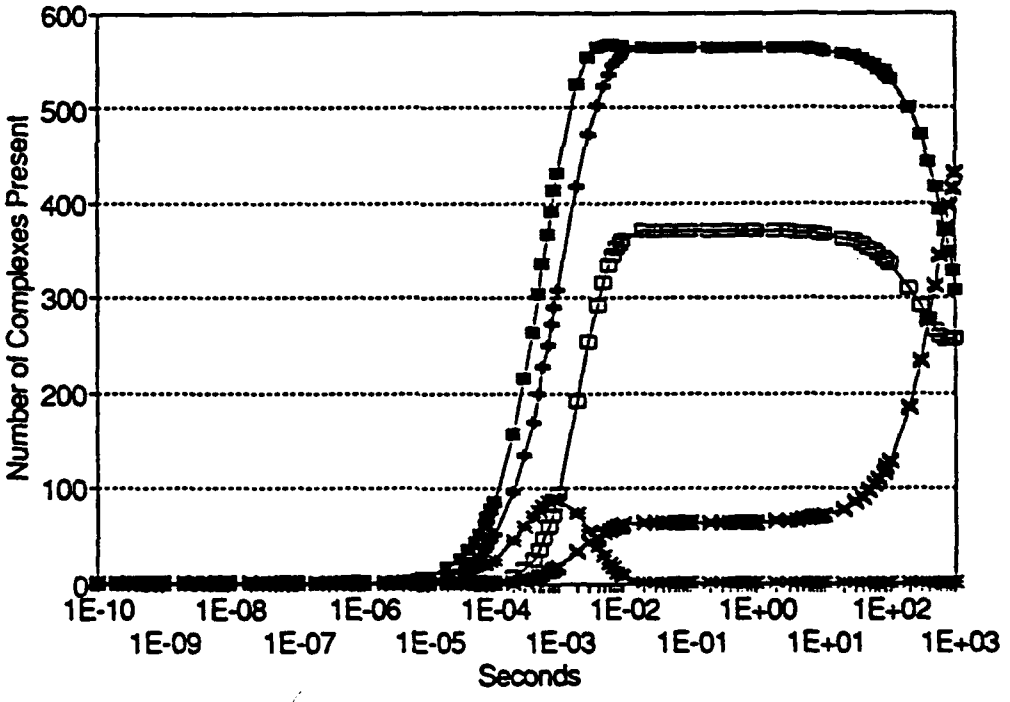
600
500
400
300
200
100
0
Number of Complexes Present
1E-10
1E-09
1E-08
1E-07
1E-06
1E-05
1E-04
1E-03
1E-02
1E-01
1E+00
1E+01
1E+02
1E+03
Seconds

Figure 13B

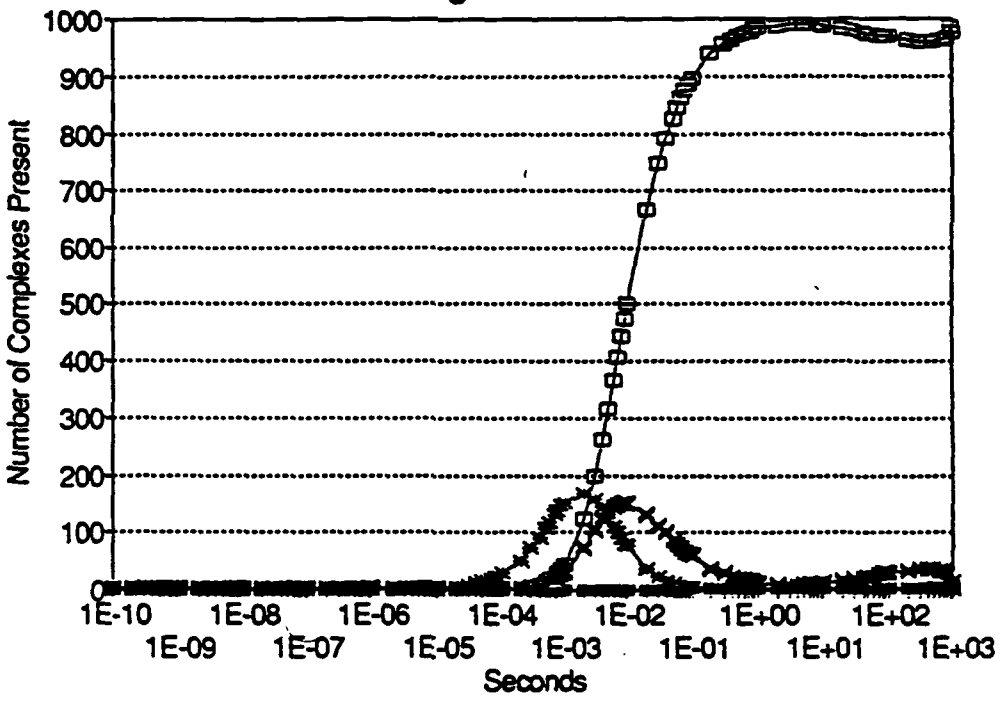
Number of Complexes Present
1000
900
800
700
600
500
400
300
200
100
0
1E-10
1E-09
1E-08
1E-07
1E-06
1E-05
1E-04
1E-03
1E-02
1E-01
1E+00
1E+01
1E+02
1E+03
Seconds

Figure 13C

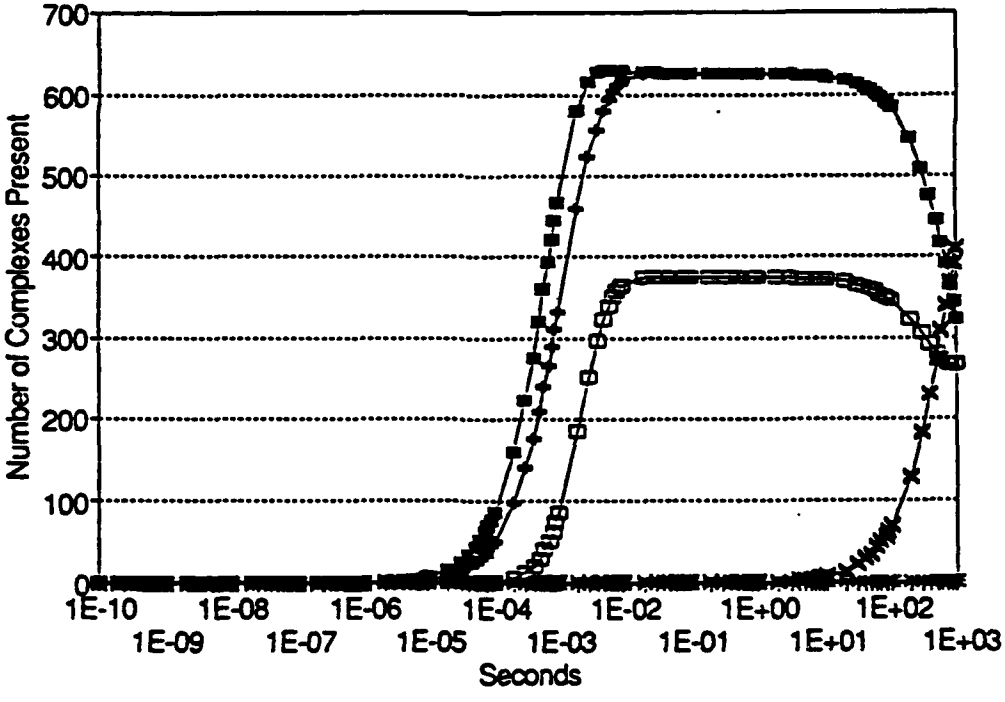
700
600
500
400
300
200
100
0
Number of Complexes Present
1E-10
1E-09
1E-08
1E-07
1E-06
1E-05
1E-04
1E-03
1E-02
1E-01
1E+00
1E+01
1E+02
1E+03
Seconds

Figure 14A

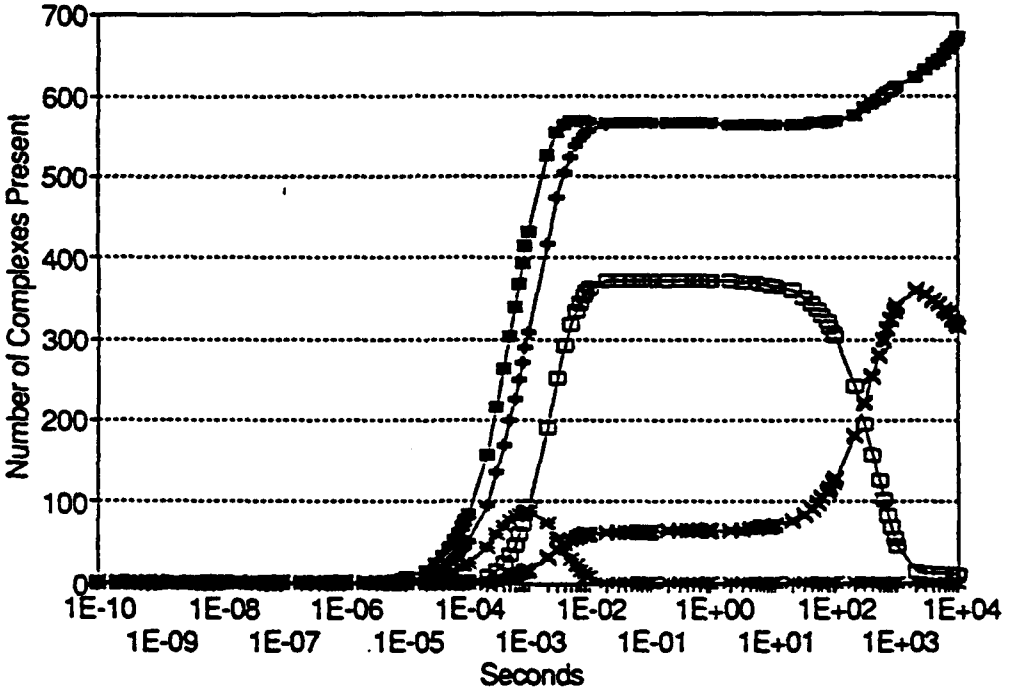
700
600
500
400
300
200
100
0
Number of Complexes Present
1E-10
1E-09
1E-08
1E-07
1E-06
1E-05
1E-04
1E-03
1E-02
1E-01
1E+00
1E+01
1E+02
1E+03
1E+04
Seconds

Figure 14B

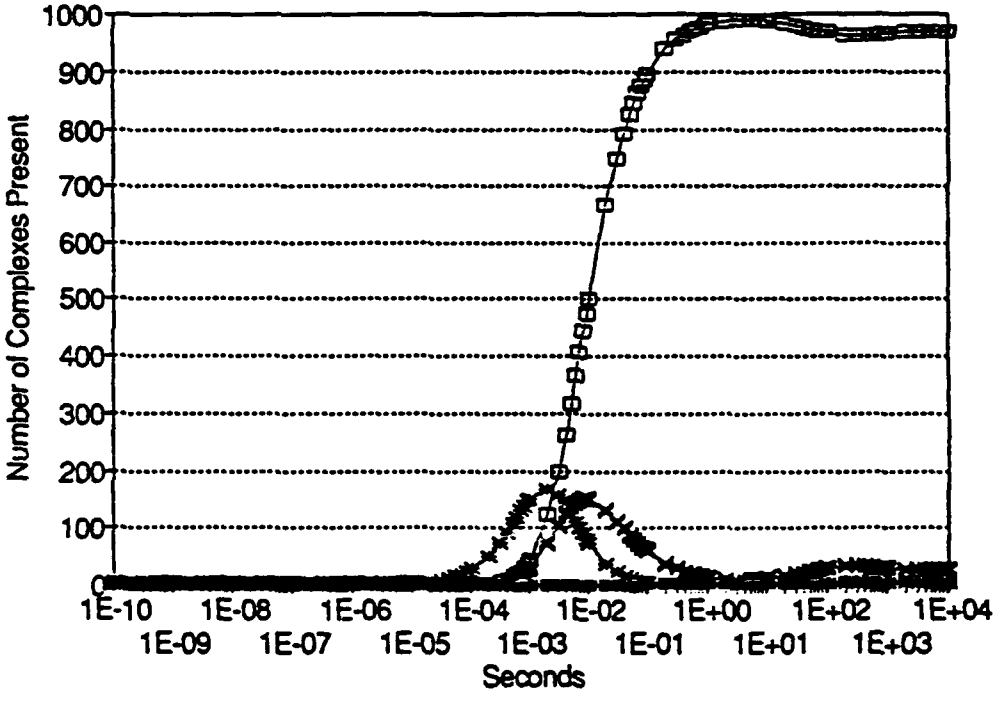
Number of Complexes Present
1000
900
800
700
600
500
400
300
200
100
0
1E-10
1E-09
1E-08
1E-07
1E-06
1E-05
1E-04
1E-03
1E-02
1E-01
1E+00
1E+01
1E+02
1E+03
1E+04
Seconds

Figure 14C

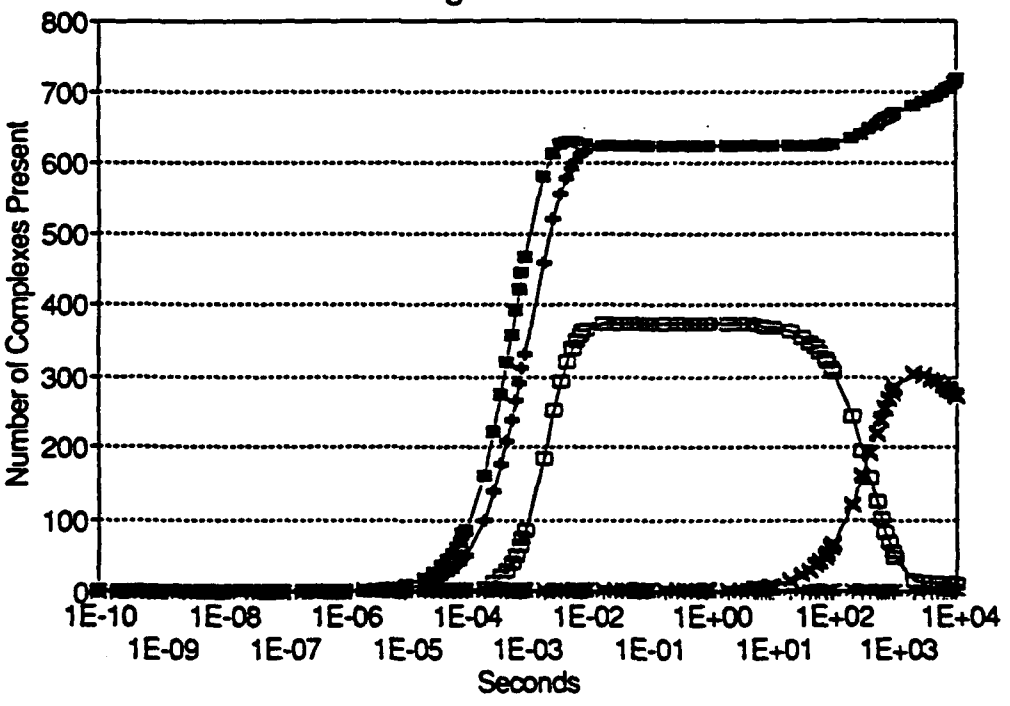
800
700
600
500
400
300
200
100
0
Number of Complexes Present
1E-10
1E-09
1E-08
1E-07
1E-06
1E-05
1E-04
1E-03
1E-02
1E-01
1E+00
1E+01
1E+02
1E+03
1E+04
Seconds

Figure 15A

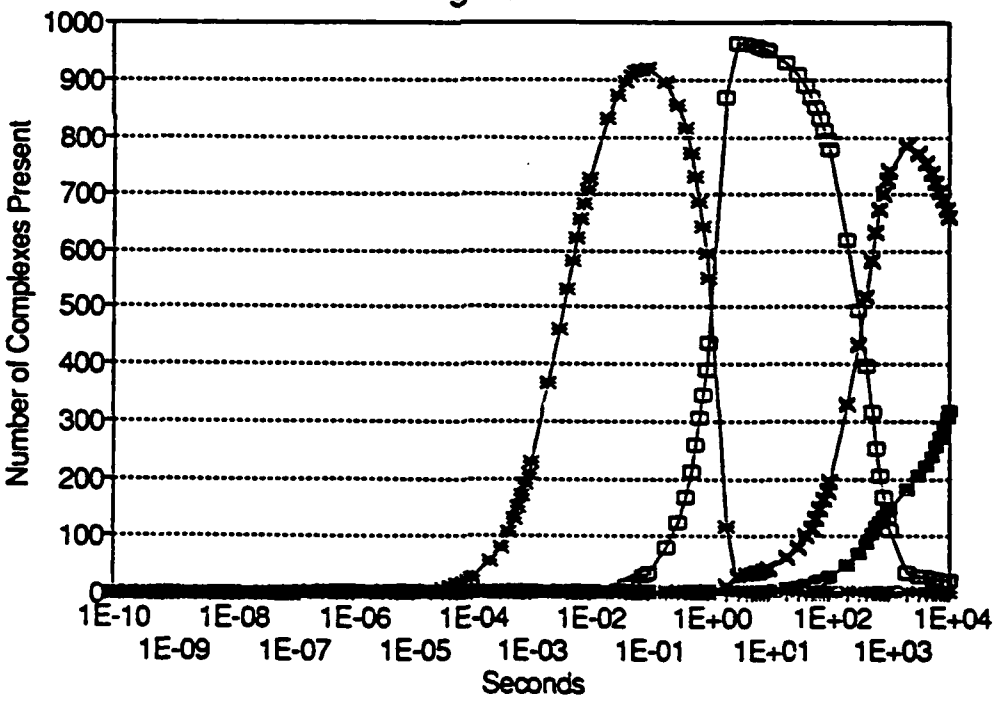
Number of Complexes Present
1000
900
800
700
600
500
400
300
200
100
0
1E-10
1E-09
1E-08
1E-07
1E-06
1E-05
1E-04
1E-03
1E-02
1E-01
1E+00
1E+01
1E+02
1E+03
1E+04
Seconds

Figure 15B

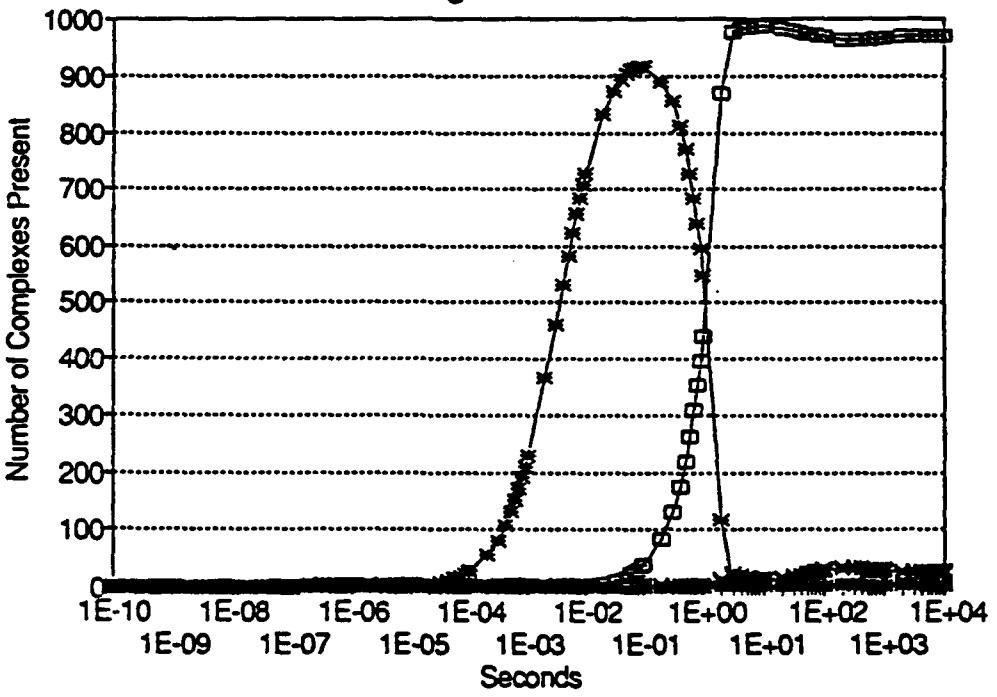
Number of Complexes Present
1000
900
800
700
600
500
400
300
200
100
0
1E-10
1E-09
1E-08
1E-07
1E-06
1E-05
1E-04
1E-03
1E-02
1E-01
1E+00
1E+01
1E+02
1E+03
1E+04
Seconds

Figure 15C

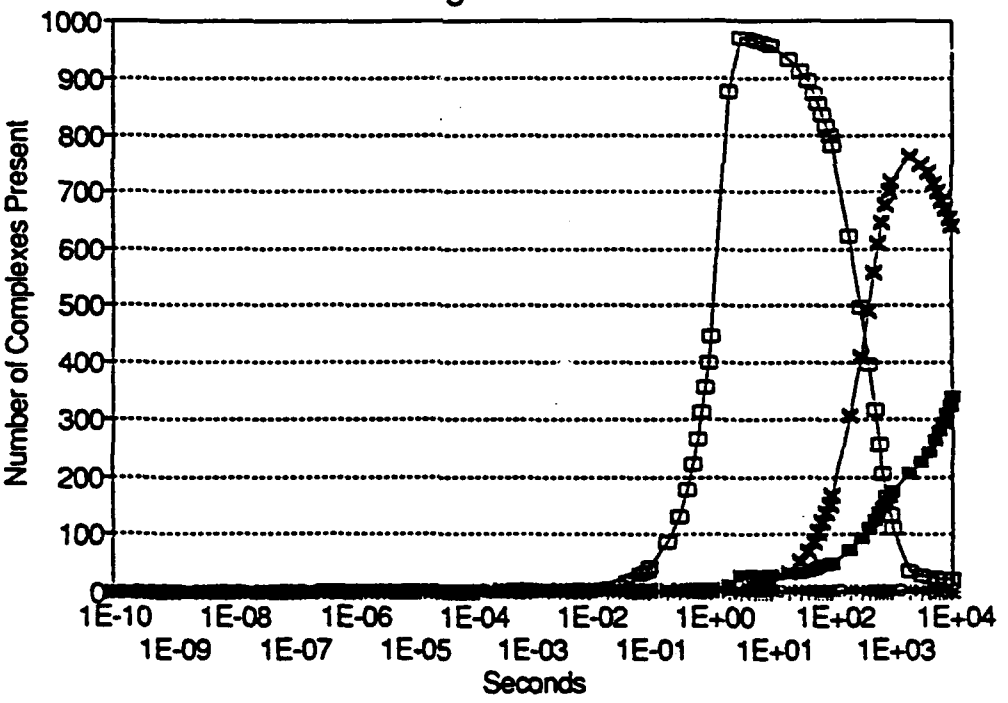
Number of Complexes Present
1000
900
800
700
600
500
400
300
200
100
0
1E-10
1E-09
1E-08
1E-07
1E-06
1E-05
1E-04
1E-03
1E-02
1E-01
1E+00
1E+01
1E+02
1E+03
1E+04
Seconds